

Autophagy orchestrates the regulatory program of tumor-associated myeloid- derived suppressor cells

Roza Maria Barouni

Principal Investigator: Panayotis Verginis

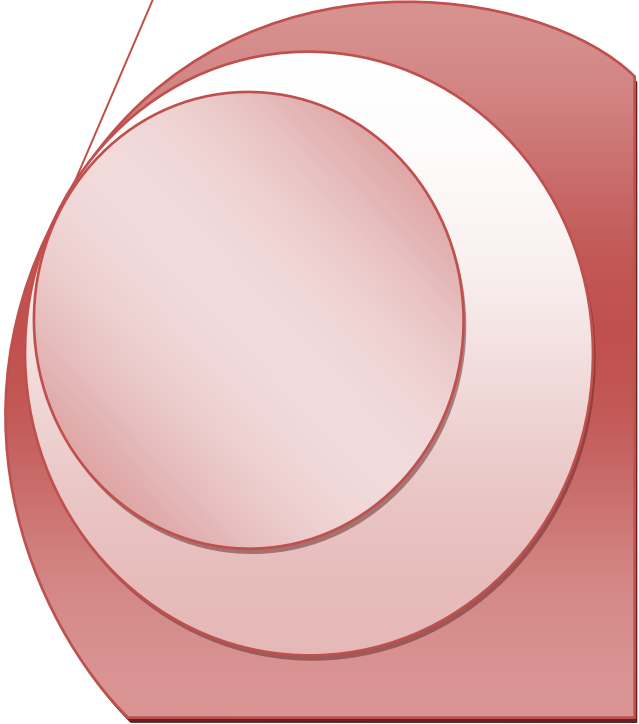
**Laboratory of Cellular Immunology and Immune
Regulation, Clinical**

**Experimental Surgery & Translational Research
Center**

**Biomedical Research Foundation of Athens
(BRFAA)**

**Graduate Program: The Molecular Basis of Human
Disease, Department of Medicine, University of
Crete**

11/17/2017



ABSTRACT.....4

INTRODUCTION.....5

MAJOR CHARACTERISTICS OF THE TUMOR CELLS 5
ONCOLOGY MEETS IMMUNOLOGY 11
MYELOID DERIVED SUPPRESSOR CELLS 13
 MDSCs subsets 13
 Expansion and activation of MDSCs in tumor 14
 Immunosuppressive mechanisms of MDSCs 16
 MDSCs in cancer..... 18
 T cells Immune Responses 19
 Antigen presentation – Major Histocompatibility Complex (MHC)..... 21
AUTOPHAGY 23
 Autophagy pathway..... 24
 The role of autophagy in Immunology 27
 Cancer and Autophagy..... 29

THESIS PURPOSE.....31

MATERIALS AND METHODS32

RESULTS40

INCREASED LEVELS OF AUTOPHAGY IN MDSCS FROM MELANOMA PATIENTS AND MELANOMA-BEARING MICE. 40
ATTENUATED TUMOR GROWTH AND INDUCTION OF POTENT ANTI-TUMOR IMMUNE RESPONSES IN MICE LACKING MDSC
AUTOPHAGY..... 44
TUMOR-DERIVED AUTOPHAGY DEFICIENT M-MDSCS EXHIBIT DIMINISHED SUPPRESSIVE ACTIVITY *IN VITRO* AND *IN VIVO*. 48
AUTOPHAGY DEFICIENCY ENCHANCES THE IMMUNOGENIC PROPERTIES OF TUMOR-DERIVED M-MDSCS. 53
ABERRANT LYSOSOMAL FUNCTION AND INCREASED ACCUMULATION OF STAT1 UP-REGULATE THE EXPRESSION OF MHC CLASS II IN
AUTOPHAGY-DEFICIENT M-MDSCS. 58

DISCUSSION63

AKNOWLEDGEMENTS66

REFERENCES.....67

Abstract

Tumor cells are characterized by specific biologic properties, which help them not only to survive and proliferate uncontrollably, but also to evade the immunosurveillance. In particular, a well characterized mechanism, used by tumor cells, is the induction of immunosuppressive cells. In other words, in the tumor microenvironment, the differentiation of an heterogeneous population, called Myeloid Derived Suppressor Cells (MDSCs), is disrupted and, thus, results in the development of pathogenic MDSCs, which contribute to the immune system suppression, and specifically in the suppression of T cells. However, the mechanisms of MDSCs mediated tumor evasion remain elusive.

In this project, we identify autophagy as a crucial pathway for MDSC-mediated suppression of anti-tumor immunity. Specifically, MDSCs in mouse tumors and melanoma patients showed increased levels of the autophagy pathway. Depletion of autophagy in myeloid compartment reduced the tumor size and enhanced the anti-tumor immune responses. Interestingly, monocytic MDSCs (M-MDSCs) exhibited impaired suppressive function both in *in vitro* and *in vivo* experiments. RNAseq of M-MDSCs, lacking the autophagy pathway showed significant differences in genes related to antigen presentation and lysosomal function. Also, autophagy-deficient M-MDSCs exhibited impaired lysosomal degradation and elevated levels of STAT1 that enhanced class II transactivator (CIITA) and MHC class II expression. Our findings depict autophagy as a novel molecular target of MDSC-mediated suppression of anti-tumor immunity.

Introduction

Cell division is a normal process, which occurs under any circumstance in almost all the tissues of an organism. Under normal conditions, the balance between the proliferation and the determinate cell death, which is usually the apoptosis, is maintained with the regulation of these two processes, in order to secure the stability of the tissues and the organs. Mutations in the genome of the cells can lead to tumor development by altering the program and the balance between the proliferation and the cell death. Subsequently, uncontrollable cell division takes place, which provokes the carcinogenesis [1].

Carcinogenesis, also called oncogenesis or tumorigenesis, is the formation of cancer, whereby normal cells are transformed into cancer cells. Especially, this process is characterized not only by changes and alterations at cellular, genetic and epigenetic level but also by uncontrollable cell division. In more details, numerous mutations in specific categories of genes are required in order to commence the oncogenesis. In other words, mutations in genes crucial for the cell division and the cell death, as also in genes related to the DNA repair mechanisms will make a cell unable to regulate its proliferation.

The abnormal cell proliferation can lead to the development of benign tumors, which do not develop, do not invade neighboring tissue or metastasize. Some benign tumors can transform to malignant neoplasms, also called cancers. Cancers develop constantly and can invade to other tissues or metastasize. The tumors that belong to this family are categorized according to the embryonic origin of the tissue that develops the tumor. Most types of cancers are characterized as carcinomas, which are the tumors that derive from endodermic or ectodermic tissues, such as the skin or the epithelium of inner organs and glands. Leukemias and lymphomas are malignant cancers of the hematopoietic cells of bone marrow. In leukemias the cells proliferate independently, while in the lymphomas, the cells create a tumor mass. Sarcomas are the less common types and are derived from mesodermal connecting tissues, such as the bones, the adipose tissue and the cartilages.

Major characteristics of the tumor cells

In brief, the hallmarks of cancer cells are practically some biologic attributes, which exist during the oncogenesis, and support the tumor development and the metastasis. (Image 1)

The normal tissues exhibit a thorough control as far as the signal production that promotes the development and the proliferation of cells is concerned. In this way, the cells maintain their homeostasis and the stability of their populations. The activating signals are transferred from growth factors that bind to their respective membrane receptors in the surface of the cells. Subsequently, the receptor activates plenty of branched-intracellular signaling pathways, which regulate the cell cycle and other functions of each cell.

The mitogenic signals, preserved in the tumor cells, are promoted by different factors. Tumor cells can produce not only the growth factors but also their receptors, in a way similar to the autocrine organs, resulting in promoting their own proliferation. Otherwise, tumor cells send signal messages to the normal cells, which then produce growth factors, useful for the development of tumor cells. Also, elevated levels of the receptors in the cell membrane of the tumor cells make them hypersensitive in the respective growth factors, even if their concentration is very low. The example above is just one of numerous ways that tumor cells use in order to maintain the proliferating signals.

1. Evading growth suppressors

Tumor cells should be able to evade signals, which have a negative regulatory feedback on their proliferation. This can be achieved through the activation of several tumor suppressive genes. A characteristic example is the retinoblastoma protein (RB) protein, which integrates signals from various extracellular or intracellular sources, and subsequently controls the cell cycle. In tumor cells, this pathway exhibits important falsies, which results in their abnormal proliferation, as RB cannot control their cell cycle. Another example is the protein TP53, which receives intracellular signals and in turn can inhibit cell cycle, or even promotes cell apoptosis. Mutations in the *tp53* gene sequence result in the constant proliferation of the tumor cells.

Furthermore, in a dense population, the cell-to-cell contact inhibits their proliferation. But, in tumor cells this contact has been abolished, resulting in maintaining their proliferation ability and creating poly-layered masses.

2. Resisting cell death

The programmed cell death, through apoptosis, is a natural barrier in the tumor growth. Specifically, apoptosis is regulated by both upstream and downstream pathways, which trigger the cell death. Tumor cells have developed numerous strategies in order to evade apoptosis. Crucial role in these strategies play the increased expression of anti-apoptotic regulators, as also the dysfunction of proteins related to apoptosis.

3. Enabling replicating immortality

Normal cells are able to proliferate successfully a finite amount of times till their death. This elimination is related to the aging process, an irreversible but viable condition, in which the cell cannot proliferate, and the cell death. Tumor cells, on the contrary, have overcome this restriction, and thus they can proliferate unaffected by the aging or cell death.

Several researches have demonstrated the pivotal role of telomeres in this phenomenon. Normal cells divisions depend on the telomeres length, as the more the length of telomeres is, the more the number of divisions of the cell are. At the same time, in normal cells, telomerase, the enzyme which adds telomere hexanucleotide repeats to the ends of the telomeric DNA, is almost absent in non-immortalized normal cells. In contrast, tumor cells dispose an active telomerase, which turns them 'immortal'.

4. Inducing angiogenesis

Tumor, as the normal tissues, requires sustenance in the form of nutrients and oxygen, and evacuation of the metabolic wastes and carbon dioxide. For this reason, it induces the angiogenesis inside its environment. The angiogenetic process is regulated by several factors, which could be either inductive or inhibitory. Some of these factors are signaling proteins, which bind to membrane receptors on the surface of endothelial cells of vessels. For example, vascular endothelial growth factor A (VEGF-A) is a characteristic factor, which expression is promoted under hypoxic conditions or by oncogenes.

5. Activating invasion and metastasis

Invasion and metastasis are two complex processes, which are compound by numerous and distinctive steps. More precisely, the pathway begins with the local invasion of tumor cells in the tissues. Afterwards, follows the intravasation of tumor cells into nearby blood and lymphoid vessels. Through those two systems tumor cells are able to transfer in the various

parts of the body, and escape towards the parenchyma of distant tissues extravasation). Then, the formation of small masses, and subsequently of the metastatic tumor follows.

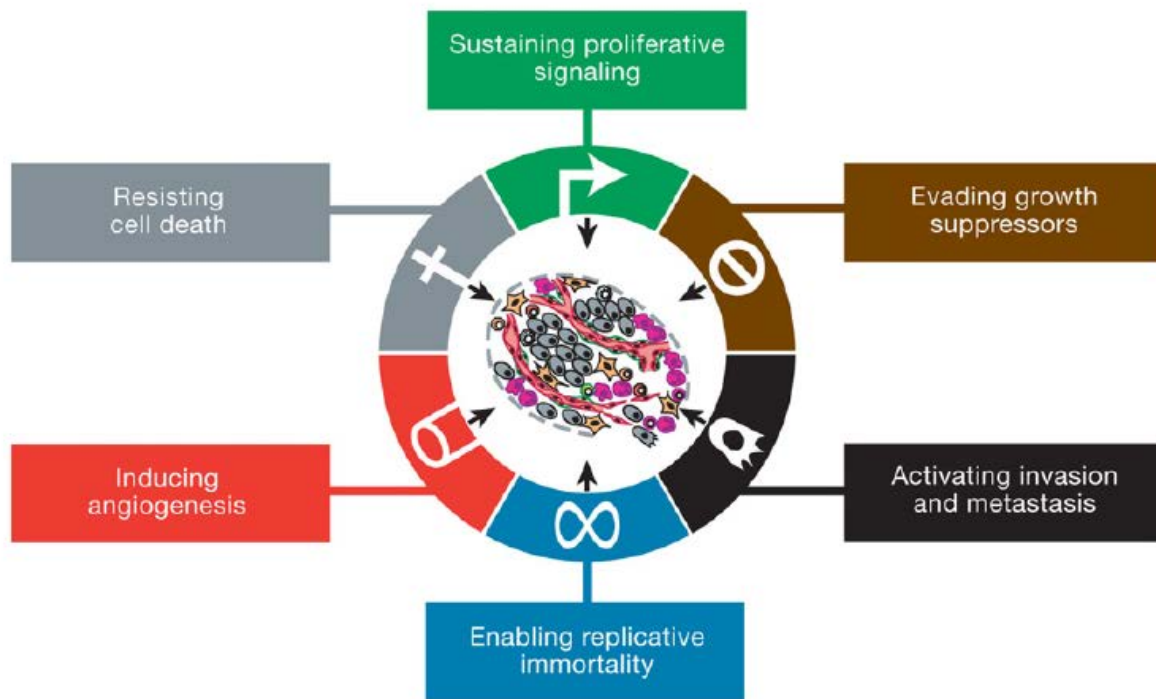


Image 1. The hallmarks of tumor cells. In the scheme the 6 main biologic properties of growing tumors are depicted. (Douglas Hanahan and Robert A. Weinberg, 2011, Cell)

6. Genome instability and mutations

Tumor cells genome is highly unstable, and that facilitates the random mutations. This results in altered genotypes of tumor cells, which give them an advantage to dominate in the local tissue environment. For this reason, tumor cells have developed mechanisms, which promote the augmentation of random mutations in the genome. These mechanisms include the increased sensitivity in mutagenic factors and the decreased effectiveness of the genomic maintenance machinery.

7. Tumor promoting inflammation

It is known that, in the tumor microenvironment, invasion by innate and adaptive immune cells takes place. This indicates the effort of the immune system to obliterate the tumor.

Neoplasms correlated with inflammatory reactions present a paradox phenomenon, in which they developed and evolved in large tumors, but simultaneously they showed all the hallmarks of the tumor cells. This is a phenomenon which is directly related to the inflammation, which releases bioactive molecules in the tumor microenvironment, such as the growth factors, that inhibit cell death, contribute to angiogenesis, to invasion in the neighboring tissues and to metastasis. Finally, inflammatory cells secrete chemical substances, like the reactive oxygen species (ROS), which play a mutagenic role and favor the tumor cells progression.

8. Reprogramming energy metabolism

The increased cell divisions and the life prolongation of tumor cells require a great amount of energy. In order to fulfill these requirements, tumor cells reprogram their metabolism. This can be achieved by increasing the glucose receptors, so that more molecules can bind to them and activate the glycolysis pathway, the one that will produce the required energy. The dependence of tumor cells on glycolysis is also demonstrated by the hypoxic conditions, in which the majority of tumor cells develops, and results in the expression of even more glucose receptors.

9. Evading tumor destruction

Immune surveillance is responsible for the recognition and the elimination of tumor cells, derived from normal cells. It is known that the immune system acts as an important obstacle in the evolution and development of cancer. Experiments on genetically modified mice, that do not have functional immune cells have revealed that tumors occur more often and develop faster compared to control mice. In more details, depletion or dysfunction of CD8⁺ cytotoxic T lymphocytes (CTLs), of CD4⁺ Th1 helper T lymphocytes or of natural killer cells (NKs) led to increased development of tumors, demonstrating the crucial role of the cell populations for the tumor elimination. (Image 2)

But, growing tumors have escaped the immune surveillance or restricted the death of tumor cells, caused by the immune cells. One step further, tumor cells have the ability to inhibit or kill the immune cells. For example, they, by secreting TGF- β , can paralyze both the CTLs and the NKs. Another mechanism used by tumor cells is the recruitment of inflammatory cells, resulting to the activation of T regulatory cells (Tregs) as also the inhibition of MDSCs differentiation [2].

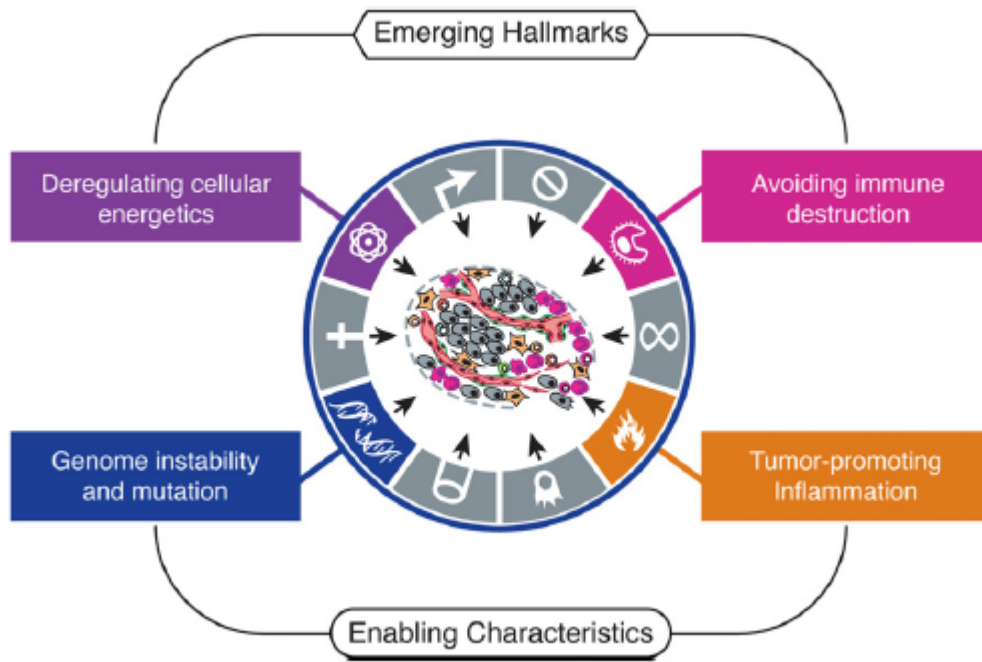


Image 2. New properties of tumor cells (Douglas Hanahan and Robert A. Weinberg, 2011, Cell)

Oncology meets immunology

Tumor cells are characterized by genetic and cellular modifications, which make the immune system able to recognize them and to activate T cell immune responses. But, the elimination of tumor by the T lymphocytes is just one step in the Cancer-Immunity Cycle (Image 3).

A series of steps should be activated and repeated, in order to characterize an immune response against tumor cells successful. These steps constitute the Cancer-Immunity Cycle. In the first step, antigens produced by the tumor cells are captured by dendritic cells (DCs) for processing. In turn, DCs present to the T lymphocytes the antigens bound to the molecules of major histocompatibility complex class I and II. This is the triggering for the activation of T cells against the tumor antigens. In this step, crucial role plays the balance between the effector T cells (Teff) and the T regulatory cells (Tregs). The activated effector T cells through the blood vessels are transferred and infiltrate the tumor area. There, the T cells recognize and bind to cancer cells by interacting specifically via their receptor (TCR) with the MHC molecules. This binding results in the death of tumor cells.

The death of tumor cells has as a consequence the further release of tumor antigens promoting the immune response anew. For this reason the above described mechanism is called cycle.

The condition, as it is elaborated above is ideal, but it is now known that its function is not the best possible. In fact, numerous mechanisms intervene and obstruct the steps of the Cancer-Immunity Cycle. Antigen presenting cells, like the DCs, may not detect the circulating tumor antigens and T cells may recognize the antigens as self-ones, and thus T regulatory cells would be activated instead of effector T cells. Also, T cells might never reach the tumor environment or their infiltration might be inhibited. Even factors that circulated in the tumor microenvironment can suppress the activated T cells. One of the most important factors that interrupt the normal prosecution of Cancer-Immunity Cycle is the suppressor cells. In this category, belong the MDSCs, which are going to be described below [3].

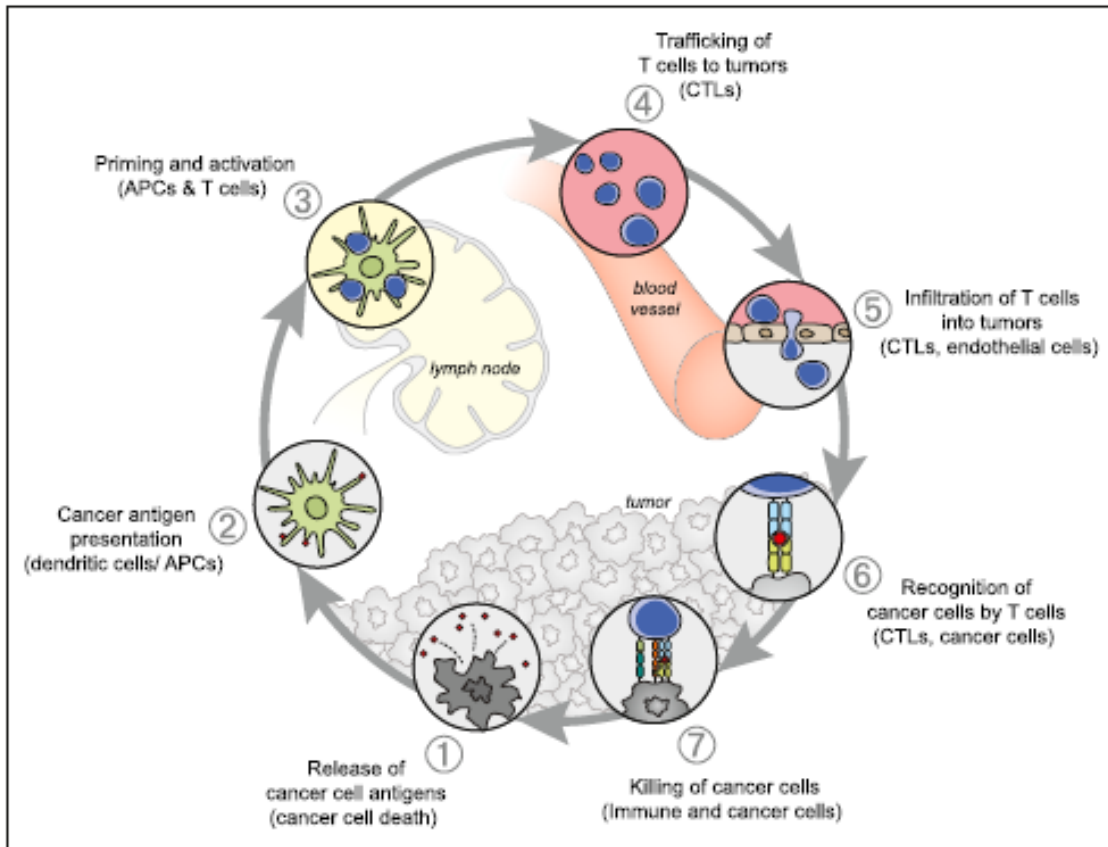


Image 3 The Cancer-Immunity Cycle. This image depicts the different steps of the immune response against the tumor cells. (Daniel S. Chen and Ira Mellman, 2013, Immunity)

Myeloid derived suppressor cells

Tumors escape the immunosurveillance, by suppressing the immune system. Although many things remain to elucidate as far as the tumor biology, the induction mechanisms and the proliferation of immunosuppressive cells are concerned, the accomplishments on the field helped to identify new immunotherapeutic targets. The current approaches in immunotherapy aim to enhance the immune system in order to kill the tumor cells and, thus, to eliminate the tumor growth. But, there are several regulatory pathways related to complex cellular interactions of the immune system that have obstructed the clinical applications and the effectiveness of the immunotherapeutic approaches against cancer. It is now known that the immune responses against tumor are negatively regulated by immunosuppressive cells, such as the T regs and the MDSCs. The latter cells are the main responsive ones for the inhibition of effector T cells against the tumor antigens and, hence, they reduce the effectiveness of the antitumor immunotherapeutic approaches.

MDSCs are a highly heterogeneous population of myeloid origin and they exhibit a huge variety among the normal and the pathological conditions. Under normal conditions these cells differentiate to DCs, Mφs and granulocytes, depending on the initial subpopulation they belong. On the contrary, in tumor environment or in other pathogenic situations, like the inflammation or sepsis, the normal differentiation pathway is interrupted and this results in the appearance of pathogenic cells with immunosuppressive properties. For this reason, these cells are called myeloid derived suppressor cells and they are defined as a heterogeneous population of immature activated myeloid cells, comprising by monocytes and granulocytes, which though do not express cell surface markers, characteristics of the fully differentiated monocytes, macrophages (Mφs) or DCs. [4]

MDSCs subsets

Under tumor conditions, the cell surface markers of the cell subsets differ among mice and humans, but even among the different types of human cancers.

In mice, MDSCs are characterized from the co-expression of two cell surface markers of differentiation of the myeloid cells, Gr-1 and CD11b (also known as Ly6C/G and M-integrins, respectively). The granulocytes have the CD11b⁺Ly6G^{high}Ly6C^{low} phenotype, while the monocytes have CD11b⁺Ly6G^{low}Ly6C^{high} phenotype. Although, the exact roles of the two populations are not fully discovered, there are evidences that demonstrate their different function in tumor and in autoimmune diseases. Both subsets expand in tumor, and especially the granulocytes. The expansion of the MDSCs subsets is not indicative of their suppressive capacity, but is characteristic of their function in the tumor microenvironment.

The respective MDSCs in humans have the CD14-CD11b+CD33+CD15+ phenotype or express the marker CD33, but not markers indicative of the mature myeloid and lymphoid cells and the major histocompatibility complex class II (MHCII). The identification and isolation of human MDSCs are difficult, due to the disparate characteristics that are present in immature stages. But, several evidences of the subsets in different types of human cancers have arisen contents among the research groups, and there is the requirement to redefine the characteristic markers for the MDSCs, due to the elevated expression levels of CD66b and the decreased levels of CD62L and CD16. It remains unclear although whether this diversity has to do with different inducible and expansive mechanisms in different types of tumors or with the use of diverse cell surface markers by the researchers [5].

Expansion and activation of MDSCs in tumor

Combined data from tumor-bearing mice and human cancers demonstrate that the induction and the proliferation of these cells in the tumor microenvironment depend on the incorporated action of multiple factors, including cytokines, growth factors and pro-inflammatory mediators. These factors can be divided into two categories: the expansion factors and the activator factors of MDSCs. The expansion, in other words the proliferation, is facilitated by a cascade of signaling molecules, which regulates the cell survival, the proliferation, the differentiation and the apoptosis. These molecules are members of the Janus tyrosine kinases family and of the signal transducer and activator of transcription 3 (STAT3). STAT3 is the main transcription factor, which is responsible for the expansion of MDSCs.

As far as the immunosuppressive function of MDSCs is concerned, it depends on the excess of the inductive and activator factors, including STAT6, STAT1 and NF- κ B, which act through multiple signaling pathways. The transcription factor STAT1 is the main factor, which is activated by the IFN- γ mediated signaling and is responsible for the increase of arginase-1 (ARG1) and iNOS expression in MDSCs inside the tumor microenvironment. These two molecules provoke the immunosuppressive function of MDSCs on the T cells. Interleukin 4 (IL-4) induces the expression of arginase-1, while the interferon- γ induces the iNOS expression in cells isolated from tumor-bearing mice (Image 4).

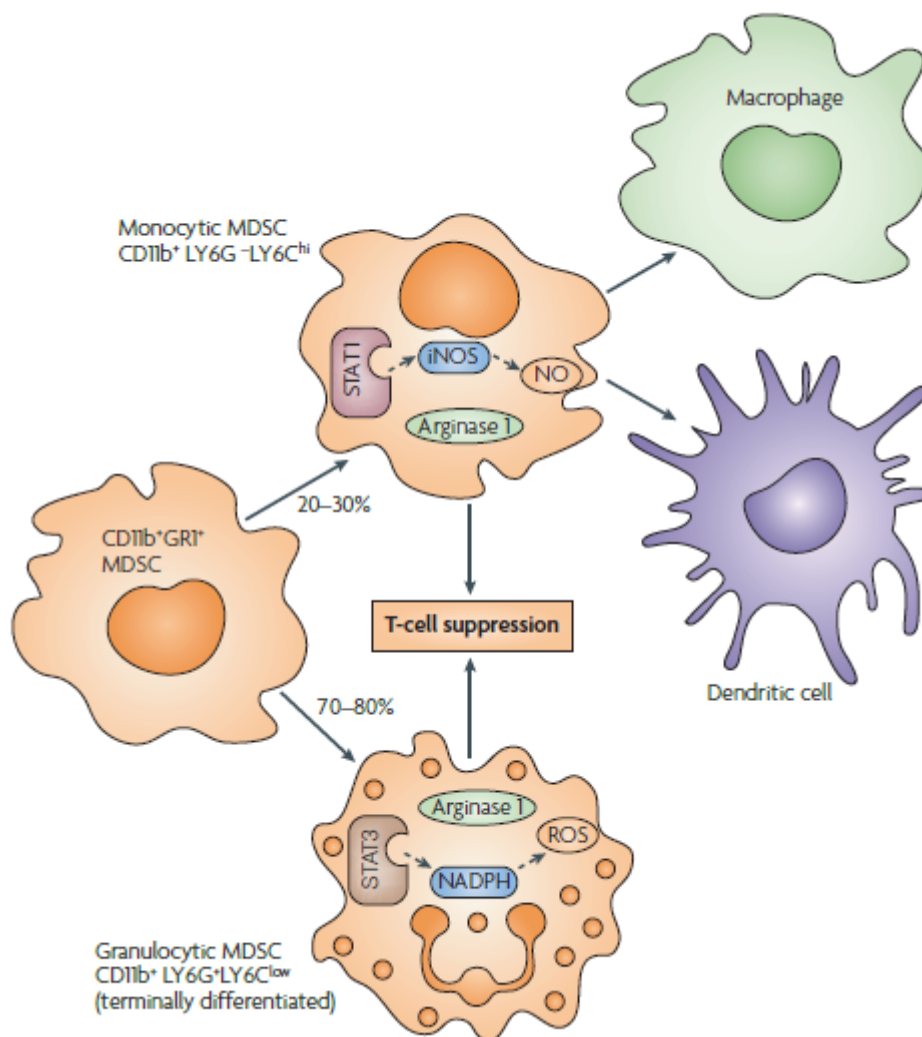


Image 4 MDSCs subsets. MDSCs (CD11b⁺Gr-1⁺) include two cell subsets, the M-MDSCs, which are characterized as CD11b⁺Ly6G^{low}Ly6C^{high} and their main transcription factor is the STAT1, and the G-MDSCs, which are characterized as CD11b⁺Ly6G^{high}Ly6C^{low} and their transcription factor is STAT3. (Dmitry I. Gabrilovich and Srinivas Nagaraj, 2009, Nature Reviews Immunology)

Immunosuppressive mechanisms of MDSCs

MDSCs mediate the induction of immunosuppression stimulated by the tumor through numerous mechanisms. It has been shown that they mediate the inhibition of T lymphocytes in cancer, through direct contact and/or combination of different mediators, like iNOS, ARG1, cyclooxygenase-2 (COX-2), prostaglandin E2 (PGE2), tumor growth factor (TGF- β), interleukin 10 (IL-10) and Tregs. These mechanisms will be further analyzed in the following paragraphs.

ARG1, iNOS and ROS

Arginase and iNOS are two distinct but correlated enzymes, expressed in high levels in these cells. They use L-arginine to produce urea and nitric oxide (NO), respectively. Elevated levels of ARG1 produced by MDSCs can accelerate the consumption of L-arginine in the tumor microenvironment, which subsequently inhibits the proliferation of T cells, as it provokes low expression of their receptor (TCR) and the cell cycle quiescence. Additionally, MDSCs suppress T cells, due to the consumption of cysteine, a crucial amino acid for the activation of T cells. These indicate that further investigation is required in order to identify new enzymes and products inside the tumor microenvironment, which are used by MDSCs so as to act negatively.

The production of reactive oxygen species (ROS) is a major regulator of the granulocytes MDSCs suppressive activity in mice models, as also in human cancers and is correlated with the tumor growth and pathogenesis. Inhibition of ROS production, in experiments, has shown reduced suppressive function in MDSCs isolated from mice and human tumors. Also, the combination of ROS and NO has been correlated with the production of hyperoxynitride, which provokes dysfunction in several proteins of target-cells and nitration of TCR, which, in turn, leads to the suppression of CD8 immune responses.

PGE2

PGE2 leads to increased levels of arginase and, hence, regulates the suppression of T cells through MDSCs. Furthermore, PGE2 promotes the recruitment of MDSCs in the tumor microenvironment through the induction of the stroma cell-derived factor (CXCL12/SDF-1), chemokines and the induction and stability of CXCL12 and CXCR4 receptors on the surface of tumor related suppressive cells.

Tumor growth factor β (TGF- β)

TGF- β is an immunosuppressive cytokine, which has been related to the function of MDSCs and the induction, as also the expansion of tumor. Experiments have shown that the main source of TGF- β production is the MDSCs, and their suppressive function is mediated by several molecules, including TGF- β . Moreover, it has been found that TGF- β promotes the evasion of tumor cells and the formation of metastasis.

T regulatory cells (Tregs)

Although it is not known whether Tregs play a role in the expansion of MDSCs, it is known that MDSCs participate in the differentiation of Tregs through the induction of several cytokines and/or the direct cell-to-cell contact. Particularly, the induction of Tregs by MDSCs depends on the presence of IFN- γ , interleukin 10 (IL-10) and on the activation by antigen-specific T cells, but it is independent of NO mechanism in tumor-bearing mice. So, MDSCs can escape the immunosurveillance with direct suppression of Tcells mediated immune responses and the induction of anergic and suppressive Tregs (Image 5).

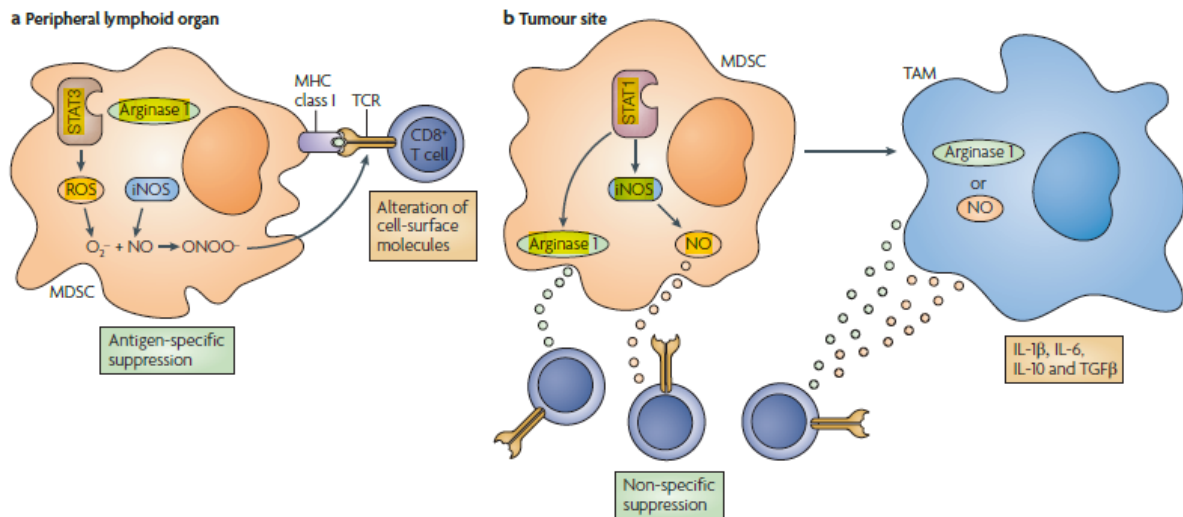


Image 5 Immunosuppressive mechanisms of MDSCs. There are two distinct mechanisms of immunosuppression. The first one involves the antigen-specific activation of Tregs, and the second one involves the non-specific soluble molecules ARG1, iNOS and ROS. (Dmitry I. Gabrilovich and Srinivas Nagaraj, 2009, Nature Reviews Immunology)

MDSCs in cancer

The effect that MDSCs exhibit in cancer can be described as the result of two distinct stages: the first includes the abnormal myelopoiesis and recruitment of these cells in the malignant tissue, while the second one is the production of cytokines by them and the interaction among the cells in the tumor microenvironment, leading to further tumor progression.

The MDSCs recruitment step is regulated by plenty soluble molecules, such as STAT3. It has been shown that the signaling pathway of TGF leads to the accumulation of MDSCs in tumor, for the purpose of escaping the immune system.

MDSCs promote the escape of tumor from the surveillance of the immune system, through the limitation of its responses and the infiltration of T cells in the tumor microenvironment. What remains to be elucidated is if the MDSCs mediate antigen-specific or not suppression of the T cell responses in the tumor.

In any case, MDSCs can ingest soluble antigens and present them in T cells, so as to provoke antigen-specific suppression.

There are results demonstrating that MDSCs isolated from tumor can suppress in a different way than the MDSCs isolated from peripheral lymphoid organs. Even though the two subsets share common morphology and phenotype, MDSCs inside the tumor express higher levels of NO and ARG1 and suppress not only the antigen-specific, but also the non specific T lymphocytes comparing to the MDSCs derived from spleen, which mediate the antigen-specific T cell suppression through the ROS pathway only.

Except of their recruitment in primitive stage in the tumor microenvironment and the promotion of the escape from immune system, MDSCs have crucial role in angiogenesis and in metastasis of tumor. In more details, they promote the expansion of tumor cells through the expression of factors that lead to a pre-angiogenic stage in the tumor microenvironment. In a melanoma-mouse model, it has been reported that MDSCs promote the expansion of tumor cells, provoking the alteration of the epithelial-mesenchymal relation. Also, the CXCL5 chemokine is the main chemokine that attracts the MDSCs in the tumor tissue. Finally, MDSCs have been correlated with tumor angiogenesis due to the production of metalloproteins (MMPs) and to the enhancement of VEGF availability [6-9].

T cells Immune Responses

An effective immune response depends greatly on the T cells action. Lymphocytes constitute a distinct type of the blood leukocytes, which is produced in the bone marrow through hemopoiesis. Lymphocytes get of the bone marrow, circulate between the blood and the lymph and colonize several lymphoid organs. Because of the express of specific membrane receptors, which

bind antigens, the lymphocytes mediate the immunologic characteristic establishment, and particularly the diversity, the immunologic memory and the self/non-self recognition. The lymphocytes are divided to two categories: the B lymphocytes and the T lymphocytes.

As it was mentioned above, the T lymphocytes are produced in the bone marrow and they migrate to thymus to mature. During the maturation, T cells begin to express on their membrane a specific antigen-binding molecule, called T cell receptor (TCR). There are now two established T subpopulations: the T helper cells (Th) and the cytotoxic T cells (Tc). These two cell populations can be distinct because of the presence of membranous glycoproteins, CD4 or CD8, on their surface. T helper cells express the CD4 marker, while T cytotoxic cells express the CD8 marker. A third subset of T lymphocytes is the one that consists by the Tregs. Tregs express CD4 on their surface, but they can be distinguished by the two former populations, as they express different cell surface markers according to their activating status.

TCR can recognize only antigens bound to the membrane proteins, called molecules of the MHC. MHC molecules are polymorphic glycoproteins on the cell surface membrane, which are divided in two types: MHC class I molecules and MHC class II molecules. The MHC class I molecules are expressed by almost all the types of nucleated cells of vertebrates, while the MHC class II molecules are expressed only by the antigen presenting cells (APCs). When an immature T cell binds to a MHC-antigen carrying molecule, it proliferates and differentiates in T memory cells and to several T effector cells. In other words, when a Th cell recognizes and interacts with the complex antigen-MHC class II, it undergoes a metabolic alteration and starts to secrete numerous cytokines. The secreted cytokines play a crucial role in the activation of B cells, T cytotoxic cells, macrophages and other types participating in the immune

response. Differences in the produced cytokines by the activated T cells lead to different immune responses [10].

Antigen presentation – Major Histocompatibility Complex (MHC)

T lymphocytes are not able to recognize soluble antigens. For this reason the antigen presentation process is necessary for their activation. This process is mediated by specific cells in the organism, named antigen presenting cells (APCs), and involves the exposure of antigen peptides in the molecules of the MHC. As it was mentioned previously, there are two categories of these molecules, the MHC class I and the MHC class II, which are correlated both in their structure and their function.

The MHC class I molecules bind peptides, which derive from endogenous and intracellular proteins that are digested in the cytoplasm, and present them to CD8⁺ T cells. These peptides are transferred from the cytoplasm to vesicles of endoplasmic reticulum (ER), where they interact with the MHC class I molecules. This process is known as cytoplasmic or endogenous pathway. MHC class I molecules are expressed by the most nucleated cells, but the expression levels differ among the distinct cell types. Cells that present peptides bound to the MHC class I molecule to the CD8⁺ T cells are referred as target cells.

The MHC class II molecules can bind also various peptides and present them to CD4⁺ T cells, but these peptides derive from exogenous proteins, which are digested through the intracellular pathway. The vast majority of peptides that bind to the MHC class II molecules, come from self membranes or extrinsic proteins, which have entered the cell through phagocytosis or endocytosis, mediated by receptors, and afterwards digestion via the intracellular pathway. In

contrast to the MHC class I molecules, the MHC class II molecules are expressed only in the antigen presenting cells (APCs) in steady levels.

Numerous cells can act as antigen presenting, but the difference consists in the ability of these cells to express MHC class II molecules and, at the same time, to provide co-stimulatory signals. Three types of cells can be characterized as professional antigen presenting cells, and these are the DCs, the M ϕ s and the B lymphocytes. These cells have differences in the antigen uptake mechanisms, the constant high expression of the MHC class II molecules and their co-stimulatory ability (Image 6).

According to the above, the antigen presenting process includes three distinct steps:

1. A pathogen or an extracellular antigen is consumed, through phagocytosis, by the antigen presenting cells and is incarcerated into vesicles. These are digested in the lysosome in order to release the antigen peptides.
2. Antigen peptides are loaded to the MHC molecules, which enter the vesicles.
3. MHC class II molecules leave the vesicles, transferring the antigens and they are lead to the extracellular membrane.
4. DCs present the antigens, which activate the T lymphocytes, when the latter bind to the MHC class II molecules [11].

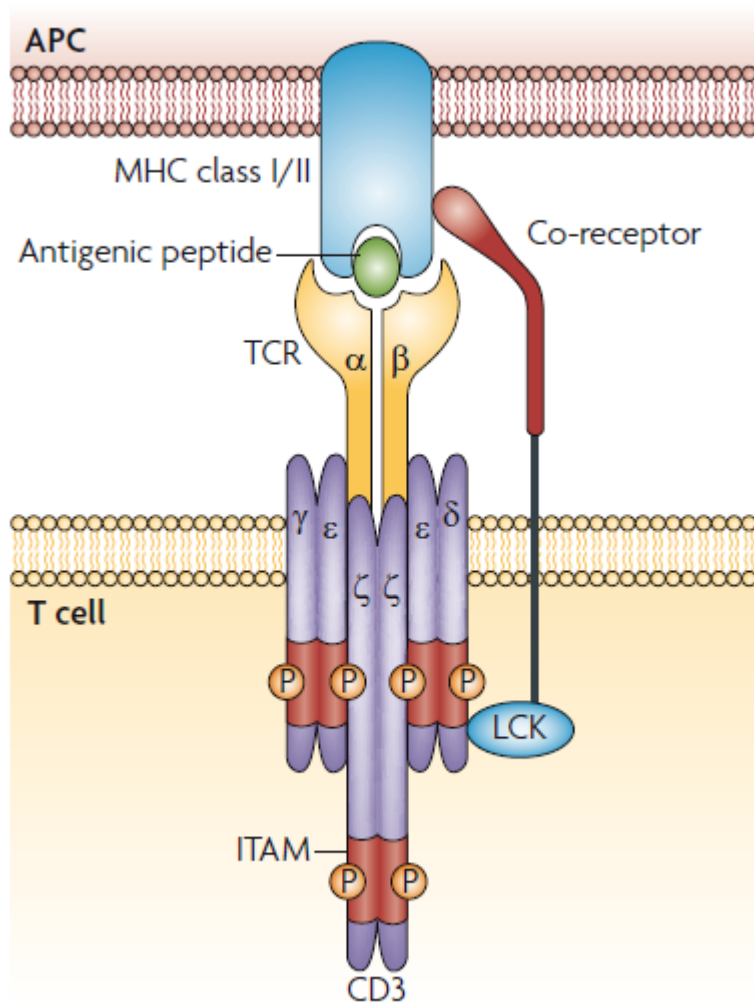


Image 6. Antigen presentation by the MHC class II molecule. The antigen peptide is presented by the MHC class II molecules of the antigen presenting cells (APCs) and is recognized by the T cell receptor (TCR). (Nicholas R. J. Gascoigne, 2008, Nature Reviews Immunology)

Autophagy

Autophagy, or autophagocytosis, is a basic catabolic mechanism, which includes the cellular digestion of useless or dysfunctional cell components, through the lysosome. The cell components digestion enables the cell survival during periods of starvation, by maintaining the energy levels in the cell.

During this process, targeted cytoplasmic components are isolated from the rest of the cell inside a membrane vesicle, which is circumscribed by a double membrane. This formation is called autophagosome, which afterwards fuses to the lysosome, creating the autophagolysosome. There, after the maturation of the autophagolysosome, the cellular contents are digested and recycled.

There are three different types of autophagy: macroautophagy, microautophagy and the chaperon mediated autophagy. The type which will be described analytically in the following paragraphs is the macroautophagy.

Macroautophagy is the main metabolic pathway for the digestion of destroyed cellular organelles and useless proteins. It depends on specific autophagy proteins, which are produced by the family of the Atg genes. Macroautophagy is a distinctive catabolic process, even from the proteasome, due to its ability to captivate and digest big targets, such as toxic inert proteins, dysfunctional and unused organelles and intruder microorganisms [12].

Autophagy pathway

The basic morphological characteristic of autophagy is the formation of intramembranic organelles, known as autophagosomes. A group of Atg factors drives the formation of the autophagic membrane of isolation, called also as phagophore, in the cytoplasm. The Beclin 1 gene, the serine/threonine protein kinase ULK1, the LC3 proteins and the gamma-aminobutyric acid A receptors (GABARAPs) are the main regulators of the phagophore formation. Phagophore originates from the phosphoinositide-3-kinase (PI3K), found on the positive areas of the endoplasmic reticulum, called omegasomes. Many more cellular organelles contribute to the phagophore formation, such as the Golgi complex and organelles derived from the mitochondrial or the cell membrane.

Recent researches have shown that autophagosomes derived from the ER, are formed in the area where ER connects with the mitochondria. Autophagy requires the spontaneous reconstruction of the intracellular membranes, which includes the temporary formation of PtdIbs3P positive structures, which come in contact with the ER, the mitochondria and the Golgi complex.

Therefore, autophagy is regulated by the serine/threonine protein kinases, ULK1 and ULK2, and by the lipid kinase of phosphoinositide-3-kinase (PI3K). This molecule forms a complex with the Beclin 1 protein and the protein, produced by the Atg14 gene. This complex in combination with the ULK1 and ULK2 proteins integrate upstream signals. These factors, which are engaged in the activation of autophagy during nutritional and immune responses, induce the downstream ATG conjugation cascade. This involves the association of ATG5-ATG12 with the ATG16L1. The complex ATG5-ATG12-ATG16L1 facilitates the addition of the phosphatidylethanolamine group to the carboxyl terminus of the mammalian paralogues of ATG-8: LC3A, LC3B (which has been used as a marker for the identification of autophagosomes in mammalian cells), LC3C, γ -aminobutyric acid receptor-associated protein (GABARAP), GABARAP-like 1 (GABARAPL1) and GABARAPL2. The modification of Atg5 by Atg12 is necessary for the prolongation of the membrane.

When the spherical structure is formed, the complex of ATG12-ATG5-ATG16L1 is digested in the autophagosome.

LC3 is disintegrated by the ATG4 protease for the creation of the cytosolic LC3. The LC3 breakdown requires the transfer and the fusion of autophagosome with the targeted-membrane. The LC3 is used usually as an autophagosome marker in immunohistochemistry, as it is the most important protein of the vesicle and remains attached on it until the fusion. Firstly, the autophagosomes fuse with the endosomes or with endosomes derived from

vesicles. These structures are called amphisomes or intermediate autophagic vacuoles and include intracellular markers. Lipid molecules combine with the above markers, contribute to the prolongation and the closure of the autophagic membrane.

The lipid kinase VPS34 via the production of the PtdIbs3P, has a double role in autophagy. This molecule is recognized by its binding factors, which in turn are activated and interact with ATG2 and ATG9 factors for the phagophore formation.

The completion of the double autophagic membrane and during the maturation process of the phagosome, a SNARE tail is appended. This tail gives to autophagosome to fuse with the lysosome (Image 7).

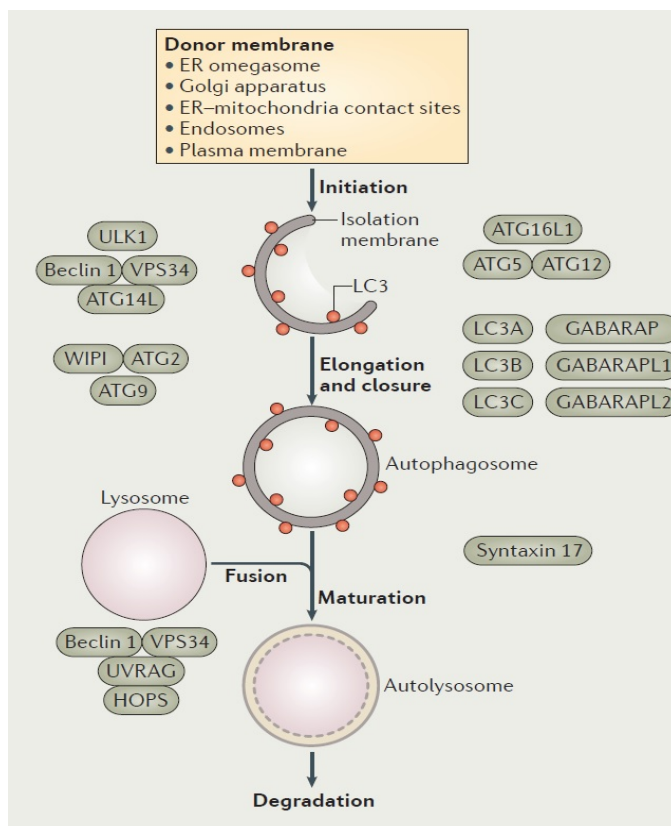


Image 7 Autophagy pathway. The autophagy pathway includes the following steps: 1. Formation of the phagophore, 2. Formation of the autophagosome, 3. Fusion of the autophagosome with the lysosome, 4. Formation of the autolysosome, 5. Protein degradation. (Deretic et. al., 2013, Nature Reviews Immunology)

The role of autophagy in Immunology

Autophagy plays an important role not only in the innate immunity, but also in adaptive immunity. In more details, its role can be divided to four distinct, which are the elimination of microorganisms, the control of pro-inflammatory signaling, the secretion of immune mediators and the effect on the adaptive immunity through regulation of the antigen presentation.

1. Elimination of microorganisms

An intrusive microorganism will activate the autophagy pathway, either due to the antagonism with the cells of the organism for the nutrients, or by activating receptors of the immune system, like the Toll like receptors (TLRs). When a microorganism is phagocytosed and remains inside the vacuole, it triggers the autophagic machinery, called LC3 associated phagocytosis (LAP), and promotes the maturation of the autophagosomes to autolysosomes.

2. Autophagy controls the pro-inflammatory signaling

Autophagy can deliver cytoplasmic molecules related to pathogens to intracellular Toll like receptors, causing their activation. Many more receptors are regulated by autophagy, which can promote the receptors augmentation, that in turn results in the increase of pro-inflammatory signaling.

3. Autophagy in the secretion of immune mediators

Autophagy affects the quality of regulated secretion of molecules, which are stored in granules. Simultaneously, autophagy affects both the quality and quantity of molecules secreted through the constitutive secretory pathway, which is the conventional pathway of protein secretion via the ER, the Golgi apparatus and the plasma membrane). Also, it supports a form of

unconventional secretion that captures cytoplasmic proteins for extracellular release.

4. Autophagy in adaptive immunity

Autophagy can increase the MHC class II molecules levels and can, also, affect directly or not the antigen presentation by MHC class I molecules. Moreover, it affects the self-renewal of the hematopoietic stem cells (HSCs), the survival of plasmocytes and the secretion of the IgG antibodies. Autophagy regulates the T lymphocytes survival, through the TCR, and destabilizes the cell-to-cell synapses. Finally, autophagy plays a role in the selection of the immature T lymphocytes in thymus, and in the survival and function of the mature T cells [13, 14] (Image 8).

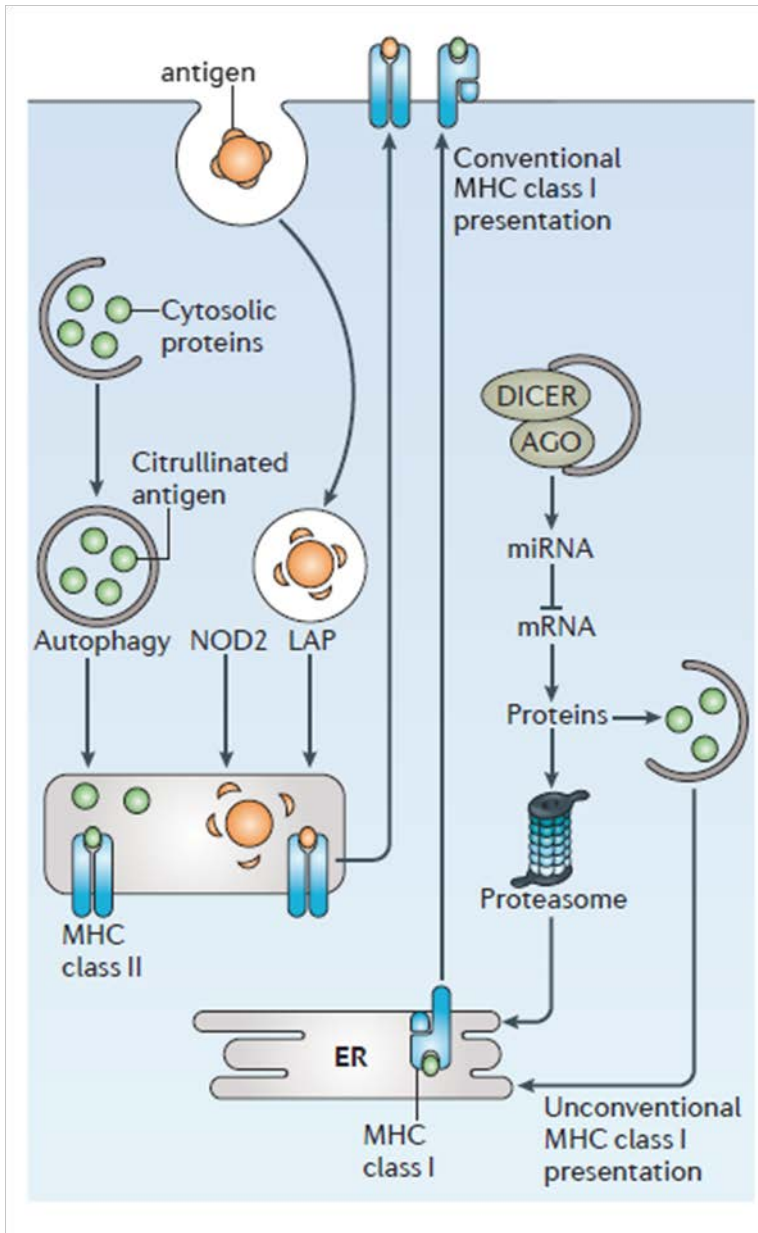


Image 8. The role of autophagy in the adaptive immunity. (Deretic et. al., 2013, Nature Reviews Immunology)

Cancer and Autophagy

Hypoxia is a normal consequence of stress that is provoked by pathological conditions, like cancer, stroke and myocardial infarction. In other words, hypoxia is the oxygen deficiency in the tissues that is caused by these conditions. In the first place, the deprivation of oxygen from the cells, will

activate adaptive mechanisms, in order to survive. If, however, the duration of the hypoxic conditions is prolonged, the certain consequence is the cell death. Cell death will be mediated by three different mechanisms: the apoptosis, the necrosis and the autophagy.

Autophagy has been related to solid tumors, like the melanoma, which will be studied in our experiments. Chronic hypoxia is characteristic of the tumor growth, which provokes the reduction of oxygen and its sources, and leads to the hypoxic conditions. These conditions cause the ATP levels to decrease, and subsequently the energy levels of the cells, as they inhibit the oxidative phosphorylation pathway. Therefore, the combination of hypoxia and low energy levels activates the autophagy pathway [15, 16].

Thesis purpose

Hypoxic conditions provoked by the tumor microenvironment, induce the autophagy pathway in the cells. Although, several studies have investigated the role of autophagy in the tumor cells, little is known about its role in the immune cells that infiltrate the tumor site.

MDSCs consist a crucial population, which can inhibit and suppress the anti-tumor immune responses with various ways, either direct or not. But it remains unclear whether these cells depend on the autophagy pathway in order to exhibit their suppressive role.

For this reason, the thesis aims to delineate the autophagy, induced by the hypoxic conditions that dominate in the tumor microenvironment, in the MDSCs and its role in the suppression that these cells exert in T lymphocytes.

Materials and Methods

Mice.

C57BL/6 mice were purchased from Jackson laboratory, *Atg5 Δ LysM* mice were generated by crossing *Atg5 $flox/flox$* mice (obtained from RIKEN BioResource Center) and *LysM cre* mice (obtained from Institute of Molecular Biology and Biotechnology institute (IMBB), OTII CD45.1 mice were kindly provided by Prof. Federica Sallusto (Institute of Research in Biomedicine, Bellinzona, Switzerland). Female mice 8-10 weeks old were used and maintained in the animal facility of Biomedical Research Foundation of Academy of Athens. All procedures were in accordance to institutional guidelines and were approved by the Greek Federal Veterinary Office.

Cell lines. The melanoma cell line B16-F10 was kindly provided by Dr. Aris Eliopoulos (Medical School, University of Crete, Greece) and the B16-F10 cell line stably expressing ovalbumin with gfp (B16-F10-OVA.GFP) was kindly provided by Dr. Caetano Reis e Sousa (The Francis Crick Institute, London, United Kingdom).

Melanoma induction.

Induction of melanoma was performed as previously described {Hatzioannou, 2016 #37}. Briefly, C57BL/6, *Atg5 Δ LysM* and *Atg5 fl/fl* mice were injected subcutaneously (s.c.) with 3×10^5 B16-F10 melanoma cells. Tumor volume was monitored from day 7 to day 15 and was calculated using the equation $(\text{length} \times \text{width}^2) / 2$.

Flow cytometry and cell sorting.

For analysis of TILs, tumors were dissected and incubated for 45 min at 37°C in RPMI medium containing 0.1 mg/ml DNaseI (Sigma), 0.2 mg/ml collagenase D (Roche). Single-cell suspensions from TILs, spleen or dLNs were stained with conjugated antibodies to mouse: CD11c (N418), Gr-1 (RB6/8C5), CD11b (M1/70), I-Ab (AF6-120.1), Ly6G (1A8), Ly6C (HK1.4), CD86 (PO3), CD4 (GK1.5), CD8 (53-6.7), CD45(30-F11), CD44 (IM7), CD80 (16-10A1), CD3 (17A2), CD25 (3C7), Va2(B20.1)(Biolegend), H-2Kb (AF6-88.5) (eBioscience) and Lysosensor (DND189) (Molecular Probes). For Foxp3 intracellular staining, cells were fixed and stained using the Foxp3 Staining Set (anti- Foxp3 clone: 150D, eBioscience Inc.) according to manufacturer instructions. For intracellular cytokine staining, CD45+ cells sorted from tumors were incubated with 50 ng/ml PMA (Sigma-Aldrich), 2 µg/ml Ionomycin (Sigma-Aldrich) and Golgi plug (1/1000) (BD Biosciences) for six hours at 37°C, and stained for IFN-γ (XMG1.2, Biolegend) using the BD Cytotfix/Cytoperm Plus Fixation/Permeabilization kit (BD Biosciences). For intracellular phospho protein staining, cells were permeabilized with the intracellular Fixation & Permeabilization buffer set (eBioscience Inc.) according to manufacturer instructions and stained with antibody against pS6 (S235/236, cupk43k) (eBioscience Inc.). CD11c-CD11b+Gr-1+, CD11c-CD11b+Ly6C+ MDSCs, CD4+CD25-Va2+ OTII T cells, CD11c+ DCs, CD3+ T cells were sorted on a FACS ARIA III (BD Biosciences). Cell purity was above 95%.

Immunofluorescence.

Cells were seeded in coverslips pretreated with poly-L-lysine (Sigma Aldrich), fixed with 4% PFA (Sigma-Aldrich) for 15 min in room temperature followed by 10 min of fixation with ice cold methanol. Cells were permeabilized by using 0.1% saponin (Sigma-Aldrich), 2% BSA and stained with mouse anti-LC3 antibody (1:20, 5F10 nanoTools), rat anti-LAMP-1 (1:400, 1D4B Santa Cruz Biotechnology), rabbit anti-p62 (1:500, MBL) and rabbit anti-STAT1 (1:300, #9172, Cell Signaling Technology) followed by incubation with Alexa fluor® 555 anti-mouse IgG (1:500, Molecular Probes), Alexa fluor® 647 anti-rabbit IgG (1:200, Molecular Probes), Alexa fluor® 488 anti-rat IgG (1:250,

Molecular Probes). For visualization of the nuclei DAPI (Sigma-Aldrich) was used. Samples were coverslipped with moviol and visualized using a 63x oil lens in inverted confocal live cell imaging system Leica SP5. Relative STAT1 intensity was calculated using Fiji software. Puncta of LC3/cell and p62/cell were calculated using a macro developed in Fiji software as described (Alissafi et al., 2017). Co-localization of STAT1 with LAMP-1 and LC3 with p62 was calculated using crosscorrelation analysis with volocity software (Costes et al., 2004).

For immunofluorescence staining of frozen tissues, tumors were embedded in OCT Tissue-Tekk specimen matrix and were cut in 7µm-thick sections using Cryostar NX50 cryotome (Thermo Fisher) at -20°C. The sections were fixed in cold acetone for 10 minutes, and were left for at least 30 minutes at room temperature. Sections were blocked with 5% goat serum in TNT buffer (20mM Tris pH 7.6, 0.9% NaCl, 0.05% Tween) for 30 minutes in room temperature and stained with rat anti-mouse CD206 (1:200, Santa Cruz, MR5D3) and rat anti-mouse CD4 (1:200, Affymetrix – eBioscience, GK1.5) either at 37°C for 1 hour in humidified chamber or at 4°C overnight, followed by staining with goat anti-rat IgG Alexa 555 (1:500, Cell Signaling) for 30 minutes at room temperature. For visualization of the nuclei DAPI (1mg/ml, 1:5000 in PBS) was used. Slides were mounted with fluorescent mounting medium (Dako) and visualized using a digital slide scanner (Zeiss Axio Scan).

All measurements were done only in the tumor area, not considering any positive signal in stroma surrounding areas. Positive area for CD206 was measured with Fiji and represented as percentage of tumor area positive for CD206. Positive cells for CD4 were counted within the tumor area and represented as number of CD4 per tumor.

Quantitative PCR analysis.

Cells were lysed in RLT buffer (Qiagen) and RNA was extracted using Qiagen RNeasy mini kit according to manufacturer instructions. First-strand cDNA synthesis was performed using Superscript II reverse transcriptase (Invitrogen). qPCR was carried out using the iTaq Universal SYBR Green Supermix (BioRad). Relative expression of target genes was calculated by comparing them to the expression of the house keeping gene *Hprt*. The following primers were used: mouse *Atg5* forward, 5'- AGCTCTGGATGGGACTG-3', *Atg5* reverse 5'- CTCCGTCGTGGTCTGAT-3', mouse *Hprt* forward, 5'- GTGAAACTGGAAAAGCCAAA-3', *Hprt* reverse, 5'- GGACGCAGCAACTGACAT-3', mouse *Ciita* forward, 5' – TGC GTGTGATGGATGTCCAG – 3', *Ciita* reverse, 5' – CAAAGGGGATAGTGGGTGTC – 3', mouse *IAb* (Qiagen).

Western Blot analysis.

Whole cell lysates from magnetically isolated M-MDSCs, were subjected to SDS - PAGE electrophoresis on 10% gels and then transferred to an Immobilon - Psq membrane (Millipore). Membranes were blocked with 5% skimmed milk, and then incubated overnight at 40C with purified mouse anti - STAT1 C-terminus polyclonal (1:1000, #9172, Cell Signaling Technology) and monoclonal mouse anti - β -actin, (clone C4 1:5000, Millipore) as a loading control. Incubation with the detection antibody of rabbit anti-mouse IgG, HRP conjugate (1:5000, Millipore) for 1 hour at RT followed. Detection was performed using Pierce ECL Western Blotting Substrate kit (Thermo Scientific).

Suppression assays.

Splenocytes from tumor bearing mice were incubated with biotin antimouse Ly6C (HK1.4, 1:200 Biolegend) followed by streptavidin microbeads (Miltenyi Biotec) and then Ly6C+ cells were positively selected on a magnetic field according to the manufacturer's instructions (MACS separation columns MS, Miltenyi Biotec). 10⁶ Ly6C+ cells from *Atg5 Δ LysM* or *Atg5 $^{fl/fl}$* mice were co-injected s.c. with 3x10⁵ B16-F10 cells in C57BL/6 mice. The tumor volume was monitored from day 7 to day 12. For *in vitro* suppression assays, highly purified M-MDSCs were sorted from tumors of *Atg5 Δ LysM* and *Atg5 $^{fl/fl}$* mice and cultured in 96-well round-bottomed plates with 1.5x10⁵ whole CellTrace-labeled (10 μ m, Invitrogen) LN cells

(LNCs) of naïve C57BL/6 mice in a 1:2 ratio, in the presence of Dynabeads mouse T-activator CD3/CD8 (Life Technologies). Cells were analyzed 4 days later.

Antigen presentation assay.

10^5 magnetically isolated Ly6C⁺ cells were cultured in 1:1 ratio with CellTrace-labeled CD4⁺CD25⁻Va2⁺ T cells isolated from OTII naïve mice in the

presence of OVA323–339 peptide (20 µg/ml, Caslo ApS). Cells were analyzed 4 days later.

Adoptive transfer experiments.

Atg5 Δ LysM and *Atg5 fl/fl* mice were implanted s.c. on the back with 3×10^5 B16-F10-OVA.GFP melanoma cells. 7 days post injection, sorted 10^6 CD4⁺CD25⁻Va2⁺ T cells from OTII naïve mice labeled with CellTrace (50µm, Invitrogen) were transferred intravenously (i.v.) and 4 days later tdLNs were isolated and analyzed.

Preparation of tumor explant supernatants (TES).

Tumors from C57/BL6 mice were dissected at day 15 and single cell suspensions were plated in 6-well plates (10^6 cells/ml). Supernatants were collected 16 hours later.

Autophagy inhibition experiments.

2.5×10^5 Ly6C⁺ magnetically isolated cells were plated in 96-well round-bottom plates and treated with LPS (1µg/ml) or tumor explant supernatants (TES 20% v/v) in the presence or absence of the inhibitors: ammonium chloride (NH₄Cl 20mM, Sigma Aldrich) and chloroquine diphosphate (CQ 50mM, Sigma Aldrich) for 16 hours.

Measurement of lysosomal function (long-lived protein degradation assay).

M-MDSCs were magnetically isolated from the spleens of B16-F10 melanoma cell-inoculated *Atg5 Δ LysM* and *Atg5 fl/fl* mice. Lysosomal function was assessed with the long-

lived protein degradation assay using [3H] leucine. In brief, 7×10^4 cells were plated in 48/well plates. 24 hours later, [3H] leucine (Perkin Elmer) was added in the culture media. The next day the medium was replaced with starvation-inducing medium and excess of unlabeled leucine. After 6 hours cells were treated with lysosomal inhibitors (NH₄Cl 20mM and leupeptin 20 μ m (Sigma- Aldrich) or bafilomycin 100 nM (Sigma-Aldrich)) or left untreated for 16 hours. For precipitation of the degraded proteins, aliquots of culture supernatants were treated with 20% trichloroacetic acid and BSA (20 mg/ml). For isolation of non-degraded proteins (proteins in media and cell lysates), cells were lysed with a mild lysis buffer containing 0.1N NaOH and 0.1 % w/v sodium deoxycholate. Counts per minute (cpm) were obtained using a beta counter. The protein degradation is calculated as degraded proteins/(non-degraded proteins + lysed cells).

RNA sequencing analysis.

M-MDSCs were isolated from the spleens of B16-F10 melanoma cell-inoculated *Atg5 Δ LysM* and *Atg5 $^{fl/fl}$* mice, using magnetic beads. RNA was extracted with Macherey-Nagel Nucleo-spin RNA kit. RNA sequencing was employed and single end 75 bp length reads were generated. Data were aligned to mouse genome (mm9) version with tophat 2 algorithm. HT-seq and DESeq algorithm were used in order to measure gene expression and identify differential expression between the two groups of patients. Genes with p-value ≤ 0.05 and fold change ≥ 1.5 or ≤ -1.5 were considered to be up- and down-regulated respectively. Gene ontology analysis, pathway annotation, transcription factor enrichment and comparison with various immunological and oncogenic gene signatures were performed with the use of DAVID knowledge base, Ingenuity Pathway Analysis software and Molecular Signature Database (MSigDB) from Broad Institute. SRA accession number: PRJNA395259.

Chromatin Immunoprecipitation assay.

5×10^6 cells were cross-linked with 1% (v/v) formaldehyde (followed by extensive wash with PBS) and lysed with 120 μ l lysis buffer (1% w/v SDS, 10 mM EDTA and 50 mM Tris-HCl, pH 8.1) and 1 \times protease inhibitor 'cocktail' (Roche), 1 mM PMSF). Chromatin was sheared using Covaris Sonicator System to 200-400 bp fragments. Supernatants were collected after centrifugation and diluted at least 5 times in Dilution Buffer (1% v/v Triton X-100, 2 mM

EDTA, 150 mM NaCl and 20 mM Tris-HCl, pH 8.1). Diluted chromatin was incubated overnight with 5 µg of normal rabbit IgG (sc-2027, Santa Cruz Biotechnology) or purified mouse anti-STAT1 (#9172, Cell Signaling Technology), followed by incubation with protein G Dynal magnetic beads (Invitrogen) for at least 3 hours at 4°C. Magnetic bead-immunoprecipitated chromatin complexes were then washed with High Salt Wash Buffer (2 times), Low Salt Wash Buffer (2 times), LiCl Wash Buffer (2 times) and TE Buffer (2 times). Chromatin was eluted from Magnetic beads with Proteinase K Digestion Buffer at 65 °C for at least 6 hours for reversal of the formaldehyde crosslinking. DNA fragments were purified with AMPure NGS magnetic beads kit (MN) and analyzed by SYBR Green Quantitative Real-time PCR. The following primer pairs were used:

ChIP_mCIITApIV_F:AGCAAACCTGGGTTGCATGT,

ChIP_mCIITApIV_R:TCCTGGCAGCTATCTCACAA

Human subjects and isolation of MDSCs from peripheral blood.

Melanoma patients (stage IV) and healthy individuals were recruited through the Oncology Department, Laiko Hospital (Athens, Greece). The Clinical Research Ethics Board approved this study and informed consent was obtained from all patients and healthy individuals prior to sample collection. Peripheral blood mononuclear cells (PBMCs) were isolated using Histopaque® 1077 (Sigma Life Science) and stained with antibodies against human CD14 (HCD14), CD33 (WM53), CD15 (W6D3) and HLA-DR (L243) (Biolegend) prior to MDSC sorting.

Statistical analysis.

Statistical analyses were performed using Student's *t* test. Two-way ANOVA statistical tests were applied in experiments with multiple comparisons. Data are presented as means ± S.E.M. Differences were considered statistically significant at $P < 0.05$. All data were analyzed using GraphPad Prism v5 software.

Results

Increased levels of autophagy in MDSCs from melanoma patients and melanoma-bearing mice.

In our first experiment we wanted to assess whether there were increased numbers of the MDSCs population in melanoma patients peripheral blood compared to the healthy donors. Our results showed that MDSCs, characterized as $\text{HLA-DR}^{\text{low/-}}\text{CD14}^-\text{CD33}^+\text{CD15}^+$, exist in higher levels in melanoma patients blood, as it is depicted in Figure 1a.

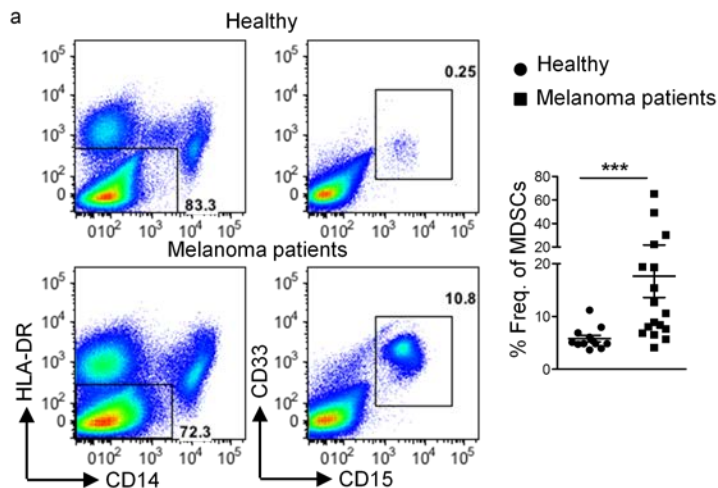


Figure 1a Gating strategy and frequencies of MDSCs ($\text{HLA-DR}^{\text{low/-}}\text{CD14}^-\text{CD33}^+\text{CD15}^+$) in PBMCs of healthy individuals (n=8) and melanoma patients (n=7) (***) ($p < 0.0001$).

Going a step further, we isolated the MDSCs population, using the specific markers, and by immunofluorescence microscopy, we defined the formation of autophagolysosomes, as it is demonstrated by the elevated expression levels of the LC3 protein and the decreased expression levels of the adaptor protein SQSTM1/p62, that targets ubiquitinated proteins for lysosomal degradation via the autophagy pathway (Figure 1b).

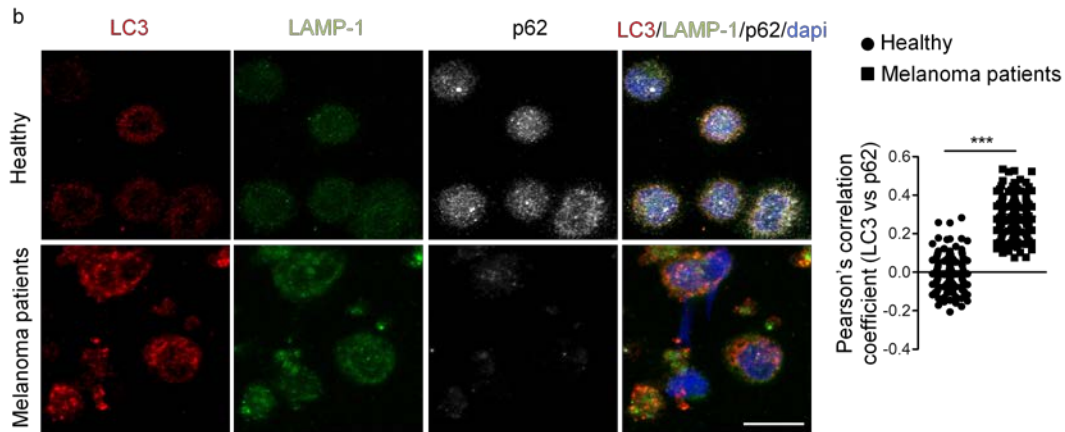


Figure 1b. Representative confocal microscopy image for LC3 (red)/LAMP-1(green) /p62 (silver white)/DAPI (blue) and Pearson's correlation of LC3 vs p62 (***p*<0.0001) in sorted MDSCs from peripheral blood of healthy individuals (n=4) and melanoma patients (n=4). Scale bar 10 μ M.

For the next experiments, we used a clinically relevant melanoma mouse model, which involves the subcutaneous injections of B16-F10 melanoma cells in C57/BL6 mice. Upon tumor establishment, MDSCs, characterized phenotypically as $CD11c^-CD11b^+Gr1^+$, in spleens of the tumor-bearing mice were significantly increased (Figure 1c).

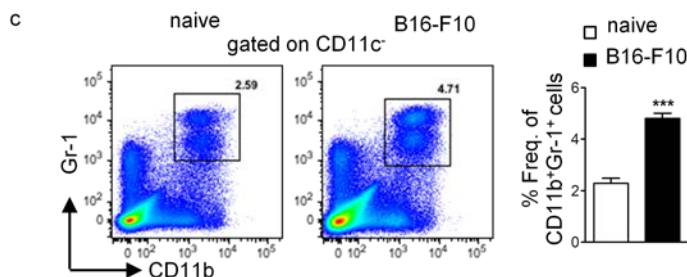


Figure 1c. Representative flow cytometric analysis and frequencies of MDSCs ($CD11c^-CD11b^+Gr1^+$) from spleens of naïve or B16-F10 inoculated mice, 10 days post-injection, (n=5 mice per group, ****p*<0.0001).

Moreover, we examined the autophagy pathway in MDSCs isolated from spleens of naïve and tumor-bearing mice and, also, by tumor sites. Our immunofluorescence microscopy results demonstrated significant increase of the LC3 protein expression, and simultaneously, significant decrease of the p62 protein expression (Figure 1d).

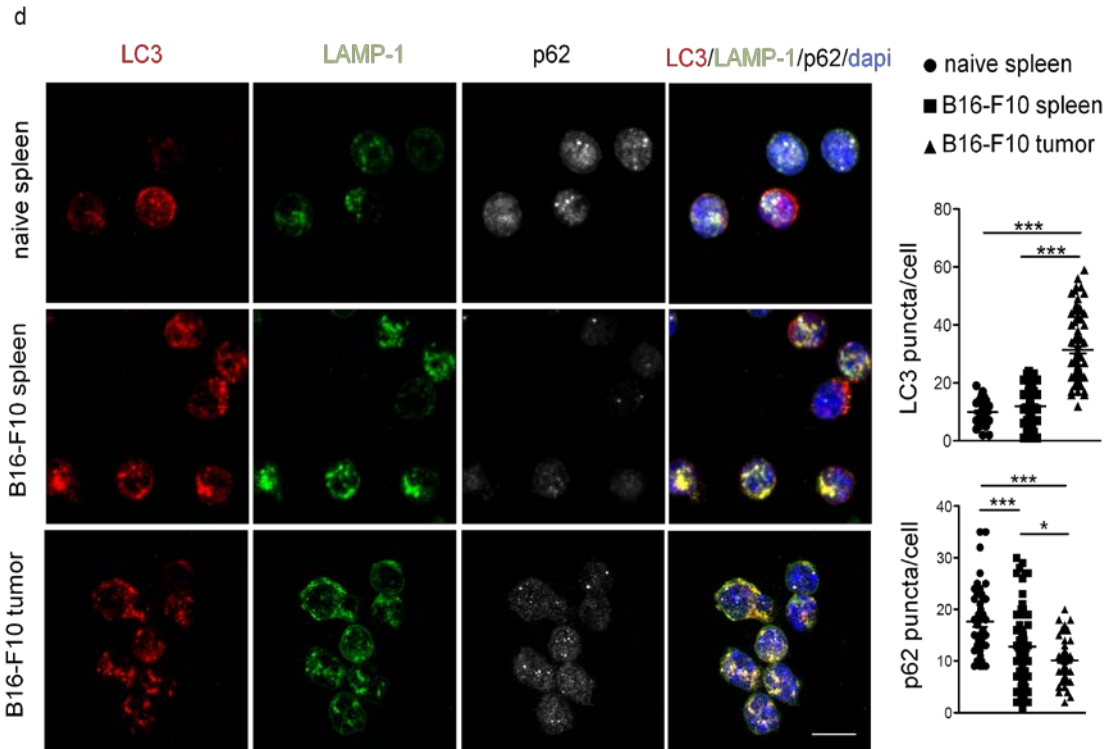


Figure 1d. Immunofluorescence confocal microscopy for LC3 (red), LAMP-1 (green), p62 (silver white), and DAPI (blue) and LC3 puncta/cell and p62 puncta/cell in sorted MDSCs from spleens and tumors of naïve and day 12 B16-F10-inoculated mice (LC3: *** <0.0001 , p62: * $p=0.0459$, *** $p=0.0003$, *** $p<0.0001$). Scale bars: 10 μm .

Finally, decreased phosphorylation of the ribosomal protein S6 (S6) was observed in MDSCs from melanoma-bearing mice compared to naïve controls indicating decreased activation of kinase mammalian target of rapamycin (mTOR) the best-characterized regulator of autophagy (Figure 1e).

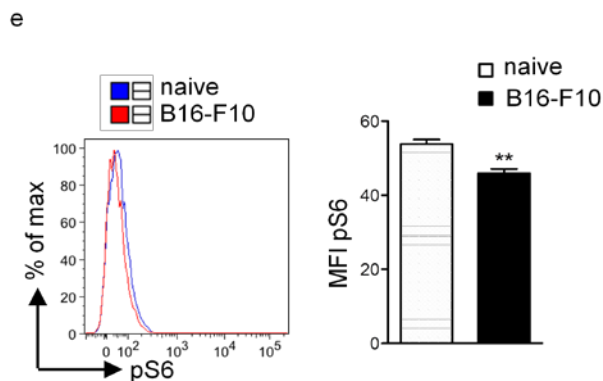


Figure 1e. Representative histogram and MFI of pS6 (** $p=0.0027$) by MDSCs from spleens of naïve or B16-F10 inoculated mice, 14 days post-injection. One representative experiment of 3 is shown. $n = 5$ mice per group.

Taking all the above data into account, it is clear that there is an up-regulation of the autophagy pathway both in MDSCs from melanoma patients and melanoma-bearing mice.

Attenuated tumor growth and induction of potent anti-tumor immune responses in mice lacking MDSC autophagy.

For the next series of experiments, we utilized genetically modified mice that do not have a functional autophagy pathway, due to the lack of *Atg5* gene from the myeloid compartment. Hereafter, these will be denoted as *Atg5*^{ΔLysM}. qPCR analysis confirmed the complete depletion of the *Atg5* gene in MDSCs, as it did not demonstrate any expression levels. Its expression levels in T cells were unaffected, whereas its expression in CD11c⁺ DCs was reduced on the half in *Atg5*^{ΔLysM} mice compared to control ones (Figure 2a). Furthermore, there was no alteration in the frequencies of the CD4⁺ and CD8⁺ cells in the thymus or in the lymph nodes of the *Atg5*^{ΔLysM} (Figure 2b, 2c).

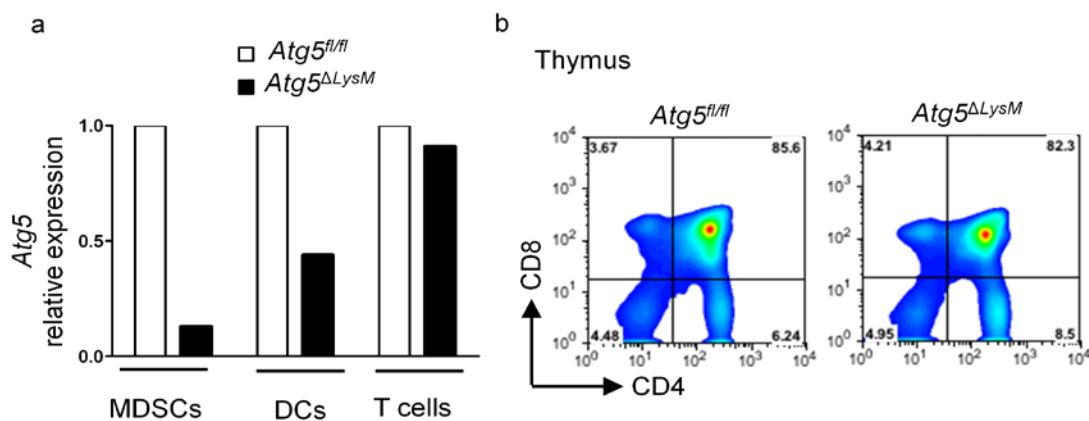


Figure 2a. *Atg5* relative expression in sorted MDSCs (CD11c-CD11b+Gr-1+), DCs (CD11c+) and T cells (CD3+) from spleens of naive *Atg5*^{ΔLysM} and *Atg5*^{fl/fl} control mice (n=3 mice/group). **3b.** Representative flow cytometric analysis of CD4⁺ and CD8⁺ T cells in the thymus of naive *Atg5*^{ΔLysM} and *Atg5*^{fl/fl} control mice (n=4 mice per group).

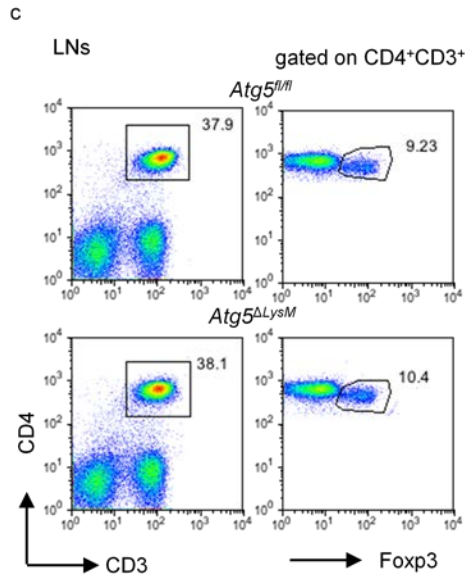


Figure 2c. Representative flow cytometric analysis of CD3⁺CD4⁺ and CD3⁺CD4⁺Foxp3⁺ T cells in the LNs of naive *Atg5^{ΔLysM}* and *Atg5^{fl/fl}* control mice (n=4 mice per group).

In order to investigate whether, there were differences in the tumor growth between the *Atg5^{ΔLysM}* mice and their control littermates, we subcutaneously injected the mice with B16-F10 melanoma cells and we monitored the tumor size from the initial stages of the tumor formation in day 8 until the day 15, when we sacrificed the mice. Interestingly, the tumors of *Atg5^{ΔLysM}* mice were significantly smaller in size comparing to the tumors of the control mice. (Figure 2d).

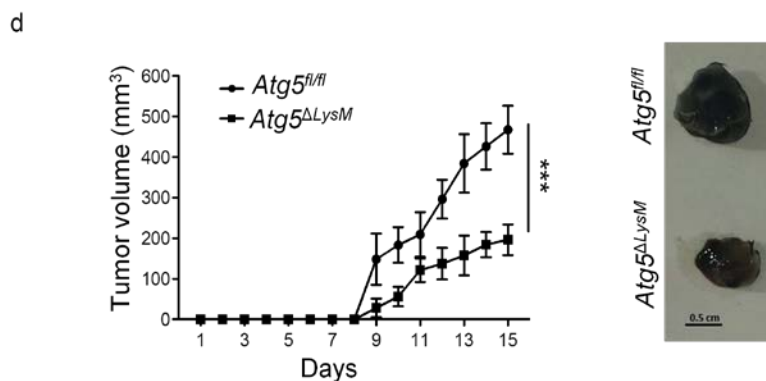


Figure 2d. Tumor volume (day 15: ***p=0.0005) and representative image of 22 excised tumors (day 13) of B16-F10 inoculated *Atg5^{ΔLysM}* and *Atg5^{fl/fl}* control mice. Representative results from three independent experiments are shown, n=5 mice per group.

Analysis of tumor-draining LNs (tdLNs) showed no differences in the frequencies of CD4⁺ and CD8⁺ T cells. However, Foxp3⁺ Tregs frequencies were significantly reduced in tumor-bearing *Atg5^{ΔLysM}* mice (Figure 2e). At the same time, analysis of tumor homogenates revealed significantly increased frequencies of CD4⁺ tumor infiltrated lymphocytes (TILs) in *Atg5^{ΔLysM}* mice, while the levels of tumor-infiltrating Foxp3⁺ Tregs were significantly reduced compared to control animals. Also, CD8⁺ TILs in *Atg5^{ΔLysM}* mice expressed increased levels of IFN- γ (Figure 2f).

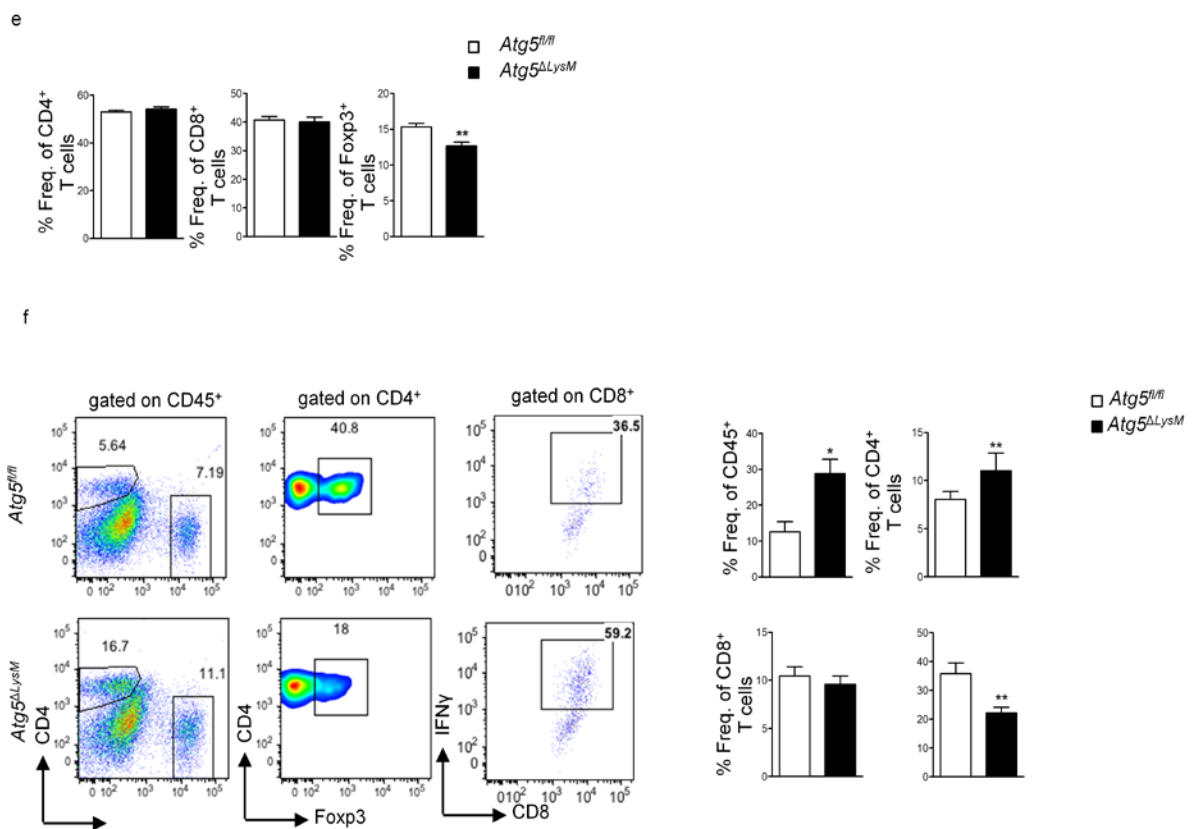


Figure 2e. Frequencies of CD4⁺, CD8⁺ T cells and CD4⁺Foxp3⁺ Tregs (**p=0.0032) in tdLNs 12-14 days after tumor inoculation in *Atg5^{ΔLysM}* and *Atg5^{fl/fl}* control mice. Representative results from four independent experiments are shown, n=10 mice per group. **2f.** Gating strategy and frequencies of CD45⁺ (*p=0.0150), CD4⁺ (*p=0.0088), CD8⁺, CD8⁺IFN γ + T cells and CD4⁺Foxp3⁺ Tregs (**p=0.0030), in tumor sites 12-14 days after tumor inoculation in *Atg5^{ΔLysM}* and *Atg5^{fl/fl}* control mice. Representative results from four independent experiments are shown, n=10 mice per group.

In addition, immunohistological analysis of tumor sites supports the increased infiltration of CD4⁺ TILs in the tumors of *Atg5^{ΔLysM}* mice (Figure 2g).

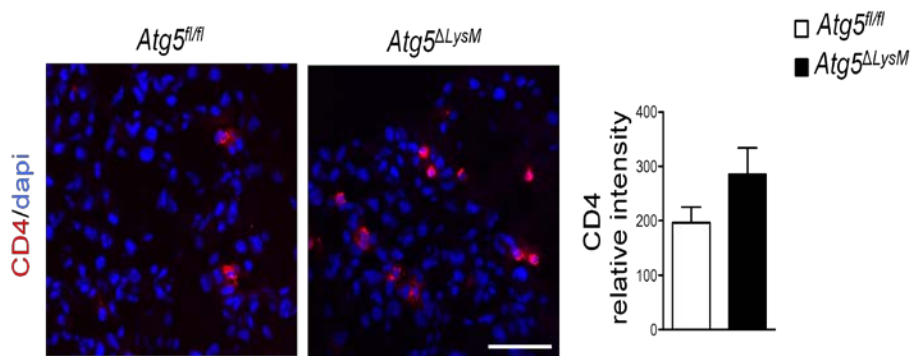


Figure 2g. Representative digital slide scanner images and number of CD4+ T cells (red) and DAPI (blue) per tumor section from B16-F10 inoculated *Atg5^{ΔLysM}* and *Atg5^{fl/fl}* control mice (day 12) are shown. n=5 mice per group, scale bar: 50 μ m.

On the whole, these results indicate that the depletion of the autophagy pathway in MDSCs lessens tumor growth and possibly plays a role in the anti-tumor response.

Tumor-derived autophagy deficient M-MDSCs exhibit diminished suppressive activity *in vitro* and *in vivo*.

With view to investigate whether the MDSC compartment has been affected by the depletion of autophagy in *Atg5^{ΔLysM}* mice, we organized the following set of experiments. Firstly, we observed increased frequencies of total MDSCs in the spleens of *Atg5^{ΔLysM}* mice, while there was no difference in the DCs population between the *Atg5^{ΔLysM}* mice and the control littermates (Figure 3a). To our surprise, the results showed a statistically significant decrease in the frequencies of the M-MDSCs subset in the spleens of *Atg5^{ΔLysM}* tumor-bearing mice, whereas the frequencies of G-MDSCs were elevated in these mice (Figure 3b).

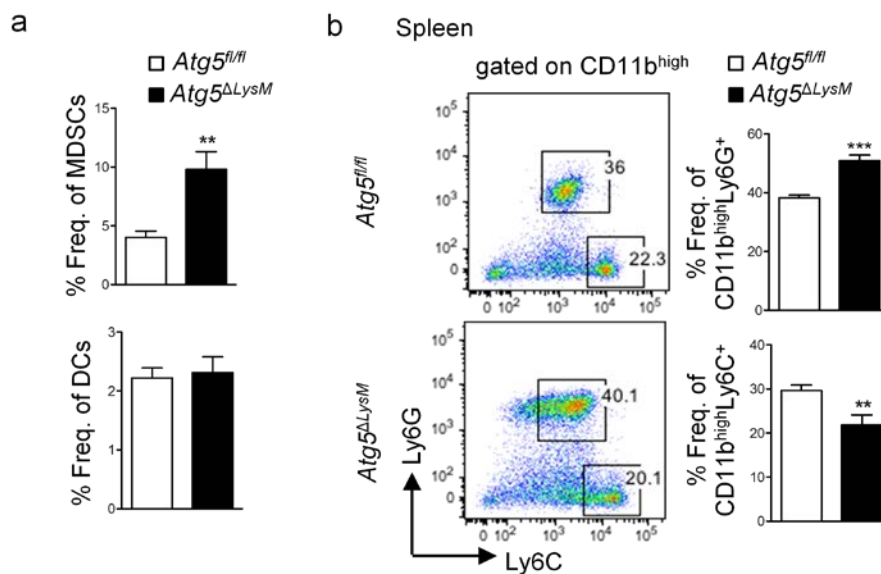


Figure 4a. Frequencies of MDSCs (CD11c-CD11b+Gr-1+) (**p=0.0036) and DCs (CD11c+) in spleens of B16-F10 inoculated *Atg5^{ΔLysM}* and *Atg5^{fl/fl}* control mice (day 13) (n=4 mice per group). **3b.** Representative flow cytometric analysis and frequencies of G-MDSCs: CD11c-CD11b^{hi}Ly6G⁺Ly6C^{low} (**p<0.0001) and M-MDSCs: CD11c-CD11b^{hi}Ly6G⁺Ly6C^{hi} (**p=0.0067) in spleens of B16-F10 inoculated *Atg5^{ΔLysM}* and *Atg5^{fl/fl}* control mice (day 13) (n=4 mice per group).

Findings concerning the behavior of MDSCs population in the tumor sites revealed that MDSCs, paradoxically, augmented (Figure 3c). As far as the subsets frequencies are concerned, we observed that there was an increased infiltration of M-MDSCs in the tumor site of *Atg5^{ΔLysM}* tumor-bearing mice, while no significant alterations were observed in G-MDSCs in *Atg5^{ΔLysM}* tumor-bearing mice comparing to the control ones (Figure 3d).

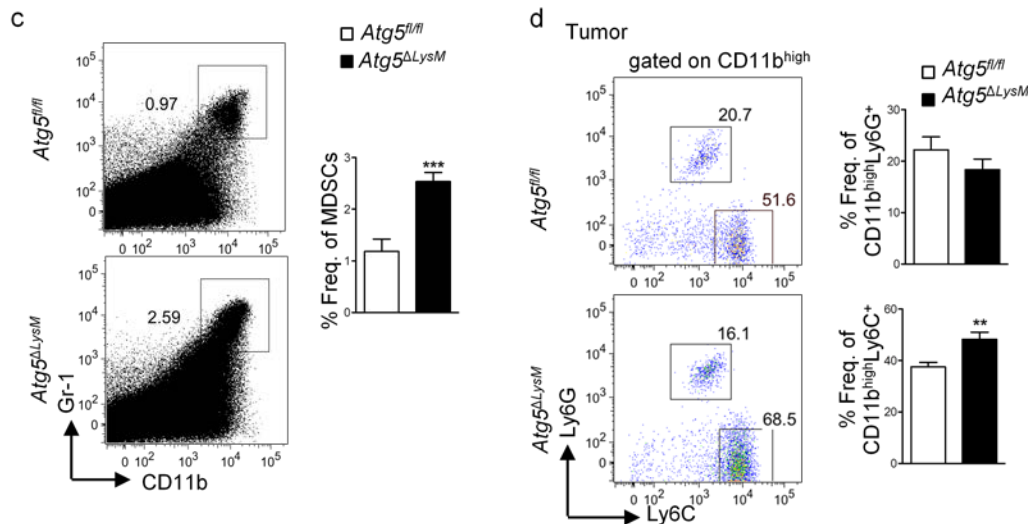


Figure 3c. Representative flow cytometric analysis and frequencies of tumor infiltrating MDSCs (**p=0.006) in B16-F10 inoculated *Atg5^{ΔLysM}* and *Atg5^{fl/fl}* control mice (day 13) (n=4 mice per group). **3d.** Representative flow cytometric analysis and frequencies of G-MDSCs: CD11c-CD11b^{hi}Ly6G⁺Ly6C^{low} and MMDSCs: CD11c-CD11b^{hi}Ly6G⁺Ly6C^{hi} (**p=0.0050) in tumors of B16-F10 inoculated *Atg5^{ΔLysM}* and *Atg5^{fl/fl}* control mice (day 13) (n=4 mice per group).

In addition, immunohistochemistry of tumor sections with CD206, which is a marker expressed by the monocytic cells, confirmed that there was increased infiltration of M-MDSCs in the tumor site of *Atg5^{ΔLysM}* tumor-bearing mice (Figure 3e).

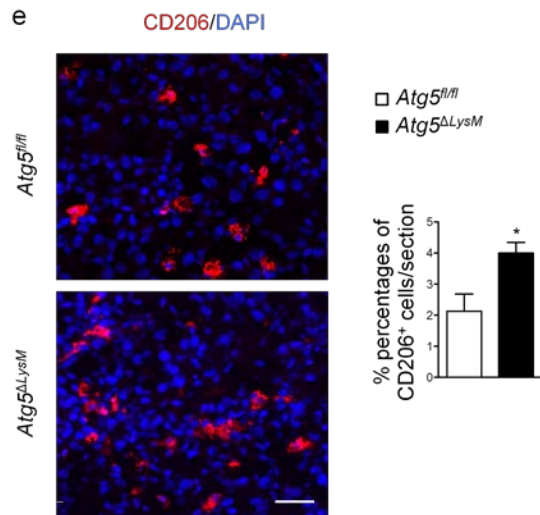


Figure 3e. Representative digital slide scanner images and percentages of CD206⁺ cells (*p=0.0310) (red) and DAPI (blue) per tumor section isolated from B16-F10 inoculated *Atg5^{ΔLysM}* and *Atg5^{fl/fl}* control mice (day 12) are shown. (n=5 mice per group, scale bar: 40μM).

The previous results prompted us to examine whether these tumor-infiltrated M-MDSCs from *Atg5^{ΔLysM}* tumor-bearing mice exhibit different functional properties compared to the infiltrated M-MDSCs of control tumor-bearing mice. For this reason we settled to sort out an *in vitro* suppression experiment with M-MDSCs derived from the tumor sites of *Atg5^{ΔLysM}* tumor-bearing mice or their control littermates and to co-culture them with total lymphocytes, stained with cell-trace violet. The results showed that M-MDSCs, isolated from the tumor sites of *Atg5^{ΔLysM}* tumor-bearing mice have lost their suppressive properties, as the T-cells could proliferate as in the control state.

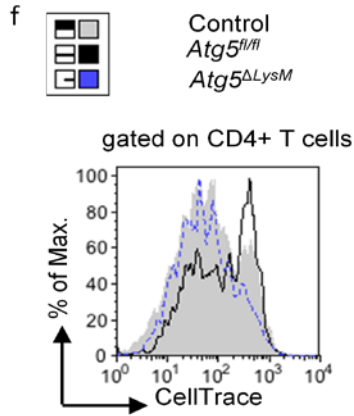


Figure 3f. Representative histogram of CD4⁺ T cell proliferation in CellTrace labeled LNCs cultured with sorted M-MDSCs from tumors of *Atg5^{ΔLysM}* and control *Atg5^{fl/fl}* B16-F10 inoculated mice at 2:1 ratio in the presence of CD3/CD28 microbeads. Representative results from two independent experiments are shown, n=4 mice per group.

Importantly, in an *in vivo* suppression model, which involved the adoptive transfer of M-MDSCs from tumor-inoculated *Atg5^{ΔLysM}* along with B16-F10 to C57/BL6 mice, significantly reduced tumor volume and tumor weight. Moreover, increased frequencies of CD4⁺ cells were detected in the tumor draining LNs, of tumor-bearing C57/BL6 mice that have received M-MDSCs from tumor-inoculated *Atg5^{ΔLysM}*. (Figure 3g, 3h)

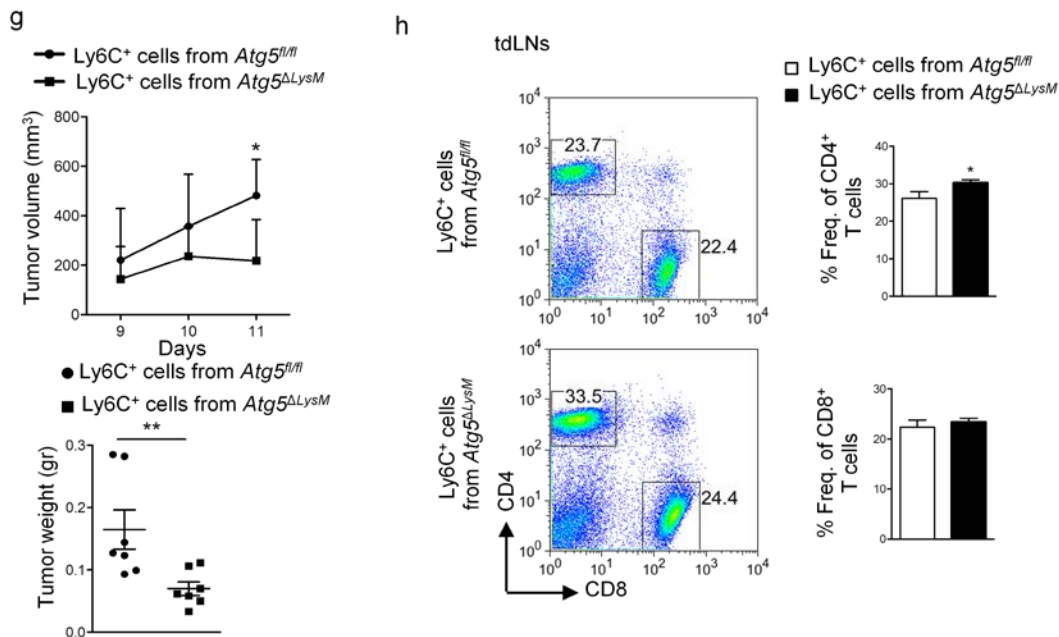


Figure 3g. Tumor volume (day 11 *p=0.0082) and tumor weight (**p=0.007) are shown. **3h.** Frequencies of CD4⁺

(*p=0.0499) and CD8+ T cells from tdLNs (day 11).

Autophagy deficiency enhances the immunogenic properties of tumor-derived M-MDSCs.

To elucidate the molecular mechanism through which autophagy dictates the suppressive activity of M-MDSCs, we performed whole genome RNA sequencing of M-MDSCs isolated from tumor-inoculated *Atg5^{ΔLysM}* and control animals. More than 1300 genes were differentially regulated in M-MDSCs from tumor-bearing *Atg5^{ΔLysM}* and control animals (Figure 4a).

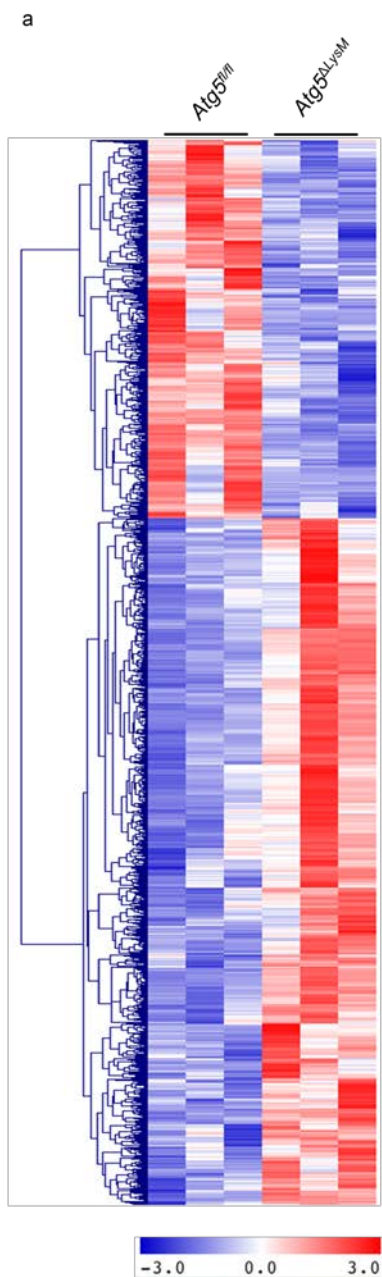


Figure 4a. Heat map of differentially expressed genes in M-MDSCs isolated from the spleens of B16-F10 inoculated *Atg5 Δ LysM* and control mice (n=3 mice/group, day 13).

Among the different analyzed clusters we focused on genes of the antigen presentation pathway (Figure 4b). qPCR confirmed that the expression of *IAb* and its transcriptional regulator class II transactivator (*ciita*) were significantly up-regulated in M-MDSCs from tumor-inoculated *Atg5 Δ LysM* mice compared to control animals indicating that absence of autophagy in M-MDSCs might augment the antigen-presenting properties of M-MDSCs (Figure 4c).

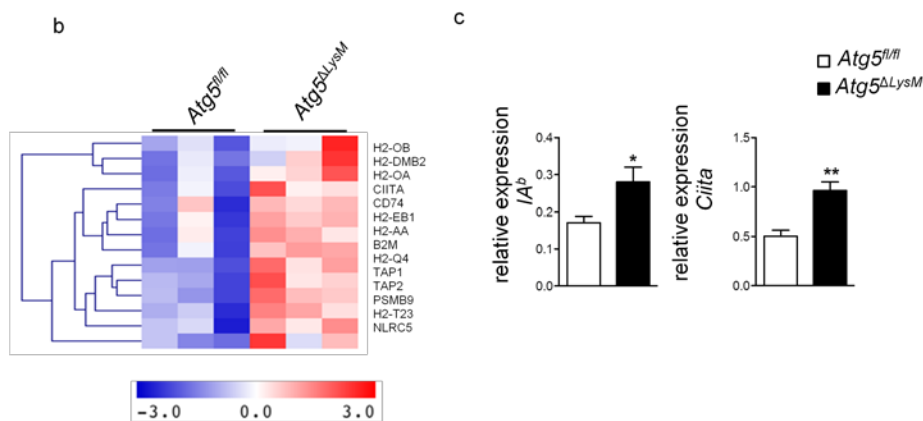


Figure 4b. Heat map of differentially expressed antigen presentation related genes of M-MDSCs isolated from the spleens of B16-F10 inoculated *Atg5 Δ LysM* and control mice (n=3 mice/group, day 13). **4c.** Relative expression of *IAb* (*p=0.0360) and *Ciita* (**p=0.0024), in sorted M-MDSCs from spleens of B16-F10 inoculated *Atg5 Δ LysM* and control mice (n=5 mice/group).

In order to test this hypothesis, concerning the antigen properties of M-MDSCs from tumor-inoculated *Atg5 Δ LysM* mice we first assessed the cell surface phenotype of these cells. The results revealed higher levels of MHC class I and II, as also of co-stimulatory molecules, such as CD80 and CD86, in M-MDSCs of tumor-inoculated *Atg5 Δ LysM* mice (Figure 4d).

d

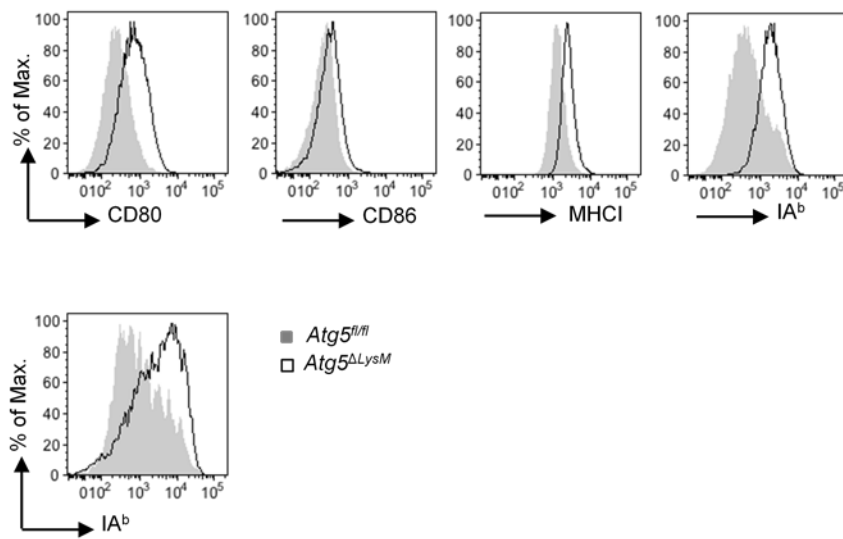


Figure 4d. Representative histograms for the expression of the indicated molecules by M-MDSCs of spleen (upper line) and tumor (lower line) of B16-F10 inoculated *Atg5^{ΔLysM}* and control mice, n=5 mice per group.

To examine whether there is a functional significance of the elevated expression levels of antigen presentation related molecules in autophagy-deficient M-MDSCs we co-cultured OVA peptide-pulsed M-MDSCs with sorted Cell-trace-labeled CD4⁺CD25⁻ OTII cells. Autophagy-deficient M-MDSCs demonstrated a superior property to induce OT II cell proliferation *in vitro* compared to WT M-MDSCs (Figure 4e).

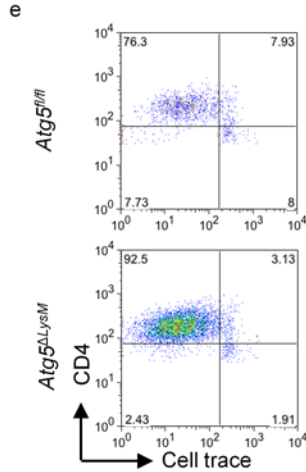


Figure 4e. Representative flow cytometric analysis for the dilution of CellTrace in OTII CD4⁺ T cells cultured with M-MDSCs isolated from spleens of *Atg5 Δ LysM* and control B16/F10 inoculated mice (1:1 ratio) in the presence of OVA peptide, n=5 mice per group.

The *In vivo* model involved the adoptive transfer of Va.2 OTII T cells into B16-F10-OVA.GFP-inoculated *Atg5 Δ LysM* mice resulted in enhanced activation (based on CD25 and CD44 expression) of the transferred OTII T cells compared to those transferred in *Atg5^{fl/fl}* animals (Figure 4f).

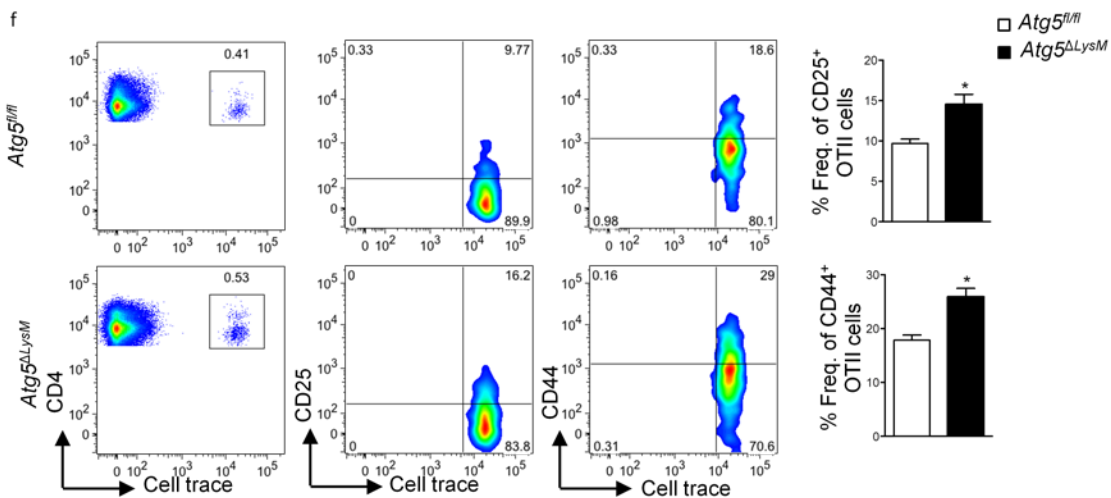


Figure 4f. Gating strategy and frequencies of CD25⁺ (*p=0.0236) and CD44⁺ (*p=0.0116) OTII CD4⁺ T cells adoptively transferred in *Atg5 Δ LysM* and control tumor bearing mice, 7 days after the tumor inoculation. Mice were sacrificed 11 days post the tumor inoculation and tdLNs were analyzed, n=3 mice per group.

Overall, these data support our theory that autophagy plays an important role in regulating the suppressive properties of M-MDSCs through up-regulation of MHC class II expression.

Aberrant lysosomal function and increased accumulation of STAT1 up-regulate the expression of MHC class II in autophagy-deficient M-MDSCs.

In order to characterize and describe the molecular mechanism which leads to the autophagy-mediated regulation of MHC class II expression in M-MDSCs isolated from tumor-bearing *Atg5^{ΔLysM}* mice. We employed network analysis of the RNAseq data, which revealed elevated expression levels of the transcription factor STAT1 in M-MDSCs from *Atg5^{ΔLysM}* tumor-bearing mice, as also a central role in the pathway (Figure 5a).

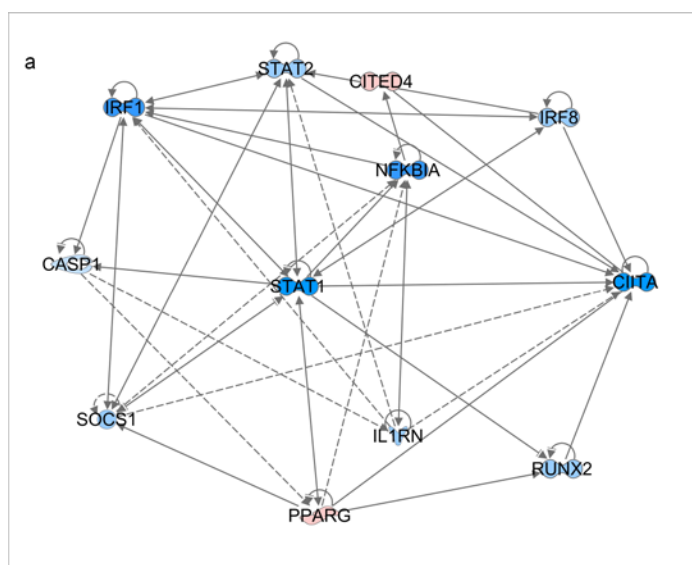


Figure 5a. Gene network analysis of *Ciita* regulators via Ingenuity Pathway Analysis (IPA) of RNA-seq dataset. (Blue and pink denote up-regulated and down-regulated genes respectively).

Furthermore, western blot analysis of protein lysates from M-MDSCs isolated from spleens of tumor-bearing *Atg5^{ΔLysM}* mice and their control littermates confirmed the increased expression levels of STAT1 (Figure 5b).

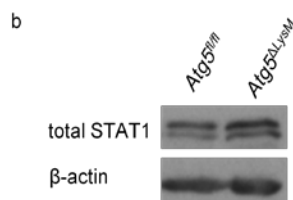


Figure 5b. Representative western blot analysis for total STAT1 and β -actin in lysates from M-MDSCs cells isolated from spleens of B16-F10 inoculated *Atg5 Δ LysM* and control mice (day 13), n=5 mice per group.

Importantly, ChIP analysis demonstrated that STAT1 binding into pIV region of proximal *Ciita* promoter was increased in M-MDSCs from *Atg5 Δ LysM* mice, indicating that higher levels of STAT1 protein is accompanied by enhanced transcriptional activation of *Ciita* target gene (Figure 5c).

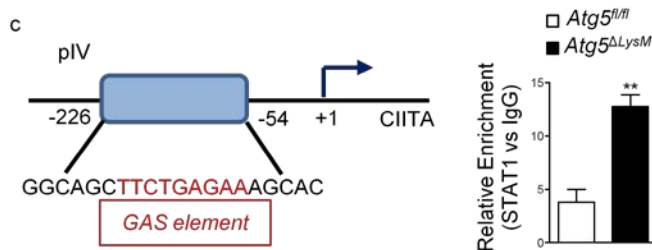


Figure 5c. Schematic representation of pIV CIITA gene proximal promoter. ChIP analysis of STAT1 binding on pIV CIITA gene promoter. (**p=0.0052).

We corroborated, also, increased protein levels of STAT1 in the cytoplasm of M-MDSCs isolated from tumor-inoculated *Atg5 Δ LysM* mice. However co-localization of STAT1 with LAMP1 showed no difference between the two groups suggesting that lysosomal degradation of STAT1 might be impaired in *Atg5 Δ LysM* mice (Figure 5d).

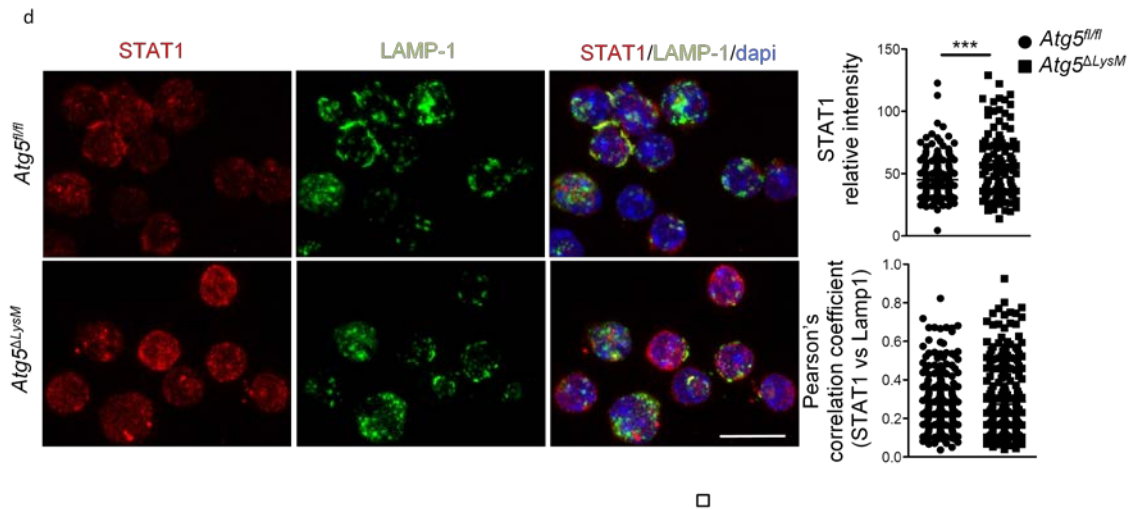


Figure 5d. Representative confocal microscopy for STAT1 (red), LAMP-1 (green) and DAPI (blue) in M-MDSCs magnetically isolated from spleens of B16-F10 inoculated *Atg5^{ΔLysM}* and control mice (day 13). STAT1 intensity (***p*<0.0001) and Pearson's correlation for STAT1 vs LAMP-1 are depicted, (n=5 mice per group).

With a view to support the above data, we analyzed the RNAseq data, which revealed a specific cluster of differentially expressed lysosomal-associated genes between the two groups of mice (Figure 5e).

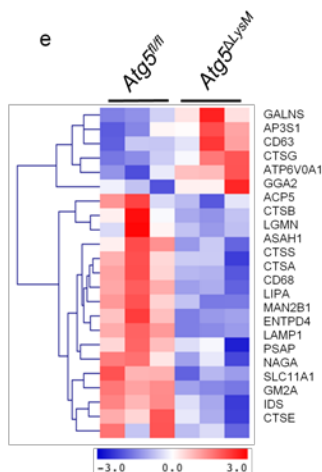


Figure 5e. Heat map of differentially expressed genes related to the lysosomal function in MMDSCs isolated from the spleens of B16-F10 inoculated *Atg5^{ΔLysM}* and control mice (n=3 mice per group).

Moreover, we examined the fluorescent levels of the LysoSensor Green (DND-189), which is a weak base that accumulates in acidic organelles and which is increased upon protonation, and we showed increased mean fluorescence intensity (MFI) in M-MDSCs from tumor-inoculated *Atg5^{ΔLysM}* mice (Figure 5f). In addition, we investigated whether the lysosomal function of the M-MDSCs, isolated from spleens of tumor-inoculated *Atg5^{ΔLysM}* mice, was impaired. In order to assess that, we used a long-lived degradation assay by pulsing M-MDSCs isolated from *Atg5^{ΔLysM}* and control mice with [³H] leucine and, indeed, the degradation capacity of lysosomes in autophagy-deficient M-MDSCs was impaired (Figure 5g).

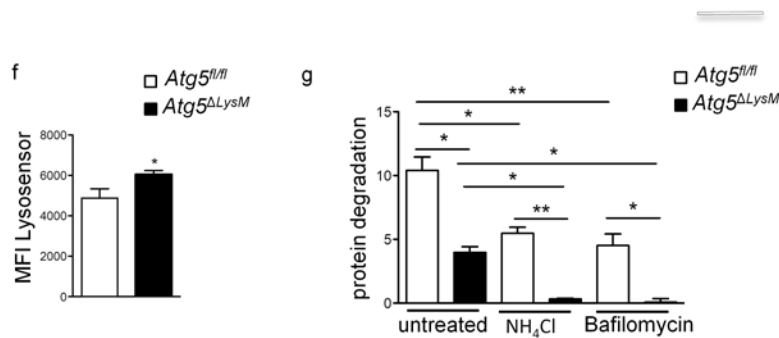
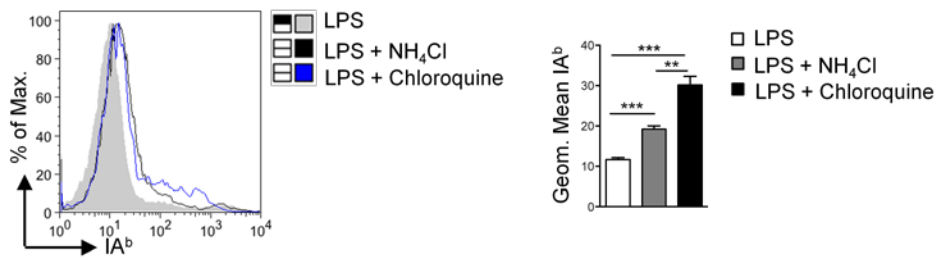


Figure 5f. MFI of lysosensor (*p=0.0470) in M-MDSCs from splenocytes of B16-F10 inoculated *Atg5^{ΔLysM}* and control mice (day 12, n=5 mice/group). **5g.** Percentage of protein degradation, using [³H] leucine, in M-MDSCs isolated from the spleens of B16-F10 inoculated *Atg5^{ΔLysM}* and control mice treated with lysosomal inhibitors (NH₄Cl and leupeptin or bafilomycin) or left untreated (n=3 mice/group). Representative results from three independent experiments are shown. (*p=0.0134, **p=0.0084, *p=0.0195, *p=0.0128, *p=0.0179, **p=0.0088, *p=0.0264).

Eventually, we performed *in vitro* blocking of the lysosomal function using NH₄Cl or chloroquine either in LPS-treated or tumor explantant supernatants (TES)-treated M-MDSCs isolated from the spleens of tumor-bearing C57/BL6 mice. The results demonstrated increased expression levels of IAb in the cell surface, which supports our hypothesis that the inhibition of the lysosomal function in M-MDSCs leads to the augmented expression of MHC class II molecules (Figure 5h, 5i).

h



i

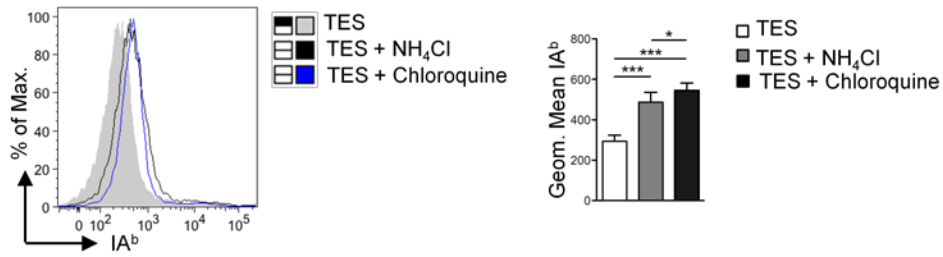


Figure 5h. Representative histograms for the expression of IA^b by M-MDSCs isolated from spleens of B16-F10 *Atg5^{fl/fl}* inoculated mice after *in vitro* stimulation with LPS (h) or TES **5i**. in the presence of NH₄Cl or chloroquine. Geometric mean of IA^b is shown, (n=5-8 mice per group (**p<0.0001, *p=0.0016)).

Discussion

Our hypothesis was based on limited knowledge concerning the role of autophagy in MDSCs in the tumor, and the lack of evidence as far as a possible direct link between the autophagy pathway and the immunosuppressive function of MDSCs is concerned. In our first results, we clearly demonstrated that the autophagy related proteins are up-regulated in the expanded MDSC population, not only in melanoma patients compared to healthy individuals, but also in melanoma-bearing mice compared to the naïve groups also. If we take into account the conditions that exist in the pathogenic situation of cancer, these results do not come as a surprise. In particular, several studies have demonstrated the up-regulation of characteristic proteins involved in the regulation and activation of autophagy. For example, the reduction of oxygen resources inside the tumor microenvironment is a factor that triggers the induction of autophagy [17]. Also, another study has revealed that HIF-1 α is the regulatory link between the reduction of oxygen and the autophagy pathway [18], and simultaneously, the expression of HIF-1 α plays a role in the MDSC differentiation [19, 20]. Moreover, hypoxia induces the up-regulation of the expression of CD45 tyrosine phosphatase activity in M-MDSCs, which lead to the decrease of STAT3 function and blocks the M-MDSC differentiation [8]. Our results target autophagy as a new pathway that its regulation could be exploited to drive MDSC differentiation and to impair their suppressive activity.

Subsequently, with view to delineate the role of autophagy in MDSCs of tumor-bearing mice, we generated a transgenic mouse model, which lacked the expression of the Atg5 protein, and thus the complete autophagy pathway from the cells of the myeloid compartment. These mice showed smaller tumors compared to their control littermates, and the immunological analysis revealed that a better immune response was taking place, because of the increased infiltration of the immune cells in the tumor sites.

As the size of the tumors was reduced, and simultaneously there was a better anti-tumor immune response, we expected that the numbers of the MDSCs in the *Atg5 ^{Δ LysM}* tumor-bearing mice would be reduced. Interestingly, the results revealed increased numbers of the total MDSC population in spleens and tumors. And as far as the subsets are concerned, the M-MDSCs subset was decreased in the spleens, but infiltrated the tumor sites in greater percentages, compared to the G-MDSCs subset, which showed the complete opposite effect. For this reason, we focused on the M-MDSCs subset in order to investigate its role and

function inside the tumor microenvironment. *In vitro* and *in vivo* experiments revealed that M-MDSCs had lost their suppressive capacity, and instead of suppressing, they promoted the proliferation of the CD4⁺ T cells. These results are highly important, as nowadays the enhancement of the anti-tumor immune responses and the increased augmentation of tumor infiltrating lymphocytes (TILs) are two of the major targets of the anti-tumor immunotherapeutic studies [21]. Another study has shown that tumor-reactive effector CD4⁺ T cells can enhance the infiltration of CD8⁺ cytotoxic T cells within tumors [22, 23]. Moreover, tumor-specific Th17 cells can inhibit melanoma growth via recruitment of DCs intratumorally and the development of anti-tumor cytotoxic T cell responses [24, 25].

This investigation, raised new questions about the mechanism, through which autophagy orchestrates the function of M-MDSCs, and whether there are alterations in the genes expression between the *Atg5^{ΔLysM}* and the control mice. The RNA seq demonstrated significant differences in various genes, and among them there were genes related to the antigen presentation machinery. Indeed, further experiments confirmed the up-regulation of the MHC class I and II molecules, as also the up-regulation of co-stimulatory molecules. Adoptive transfer experiments showed that autophagy-deficient M-MDSCs enhance the anti-tumor immune responses. Interestingly, other studies report that MDSCs express low levels of MHC not only in tumor mouse models [9], but also in patients with tumors [26, 27]. One hypothesis is that low levels of MHC expression by MDSCs would render them tolerogenic that will preferentially promote induction of Tregs. Our above results reveal a novel mechanism concerning the expression of MHC class II by M-MDSCs, mediated by autophagy. Specifically, M-MDSCs from tumor bearing autophagy deficient mice showed increased expression of STAT1 with enhanced binding to *Ciita*, which lead to increased MHC class II expression. Overall, this increased expression of MHC class II promoted the proliferation of tumor-derived antigen-specific T cells *in vivo*. At the same time, lysosomal function was severely affected in autophagy-deficient M-MDSCs and *in vitro* blocking of lysosomal compartment significantly increased MHC class II expression. Early studies showed that DCs with limited lysosomal proteolysis are more potent APCs than macrophages with high proteolytic capacity [28]. The mechanism through which autophagolysosomes might regulate MHC expression remains elusive. A sufficient explanation would be that due to the dysfunction of the autophagolysosome, the proteins escape and do not sustain to degradation. In turn, this provokes changes in the proteins expression in M-MDSCs, resulting in increased levels of STAT1 that subsequently enhances CIITA transcription.

Collectively, autophagy has been shown to exhibit either beneficial or negative effects in tumorigenic events [29, 30], but its role in shaping the function of tumor-associated immune regulatory cells remained obscure. Our findings demonstrate that autophagy plays a crucial role in the differentiation of M-MDSCs to suppression cells that promote tumor growth. Targeting autophagy therapeutically could enhance the activation and the expansion of effector CD4⁺ T cell and to trigger anti-tumor immune responses. Currently a large number of clinical trials targeting autophagy in cancer have been launched [31] in combination with chemotherapy or other targeted agents. However, the generalized effect of autophagy inhibition in the development of an anti-tumor immunity remains obscure and deems further investigation.

Aknowledgements

Firstly, I would like to thank Dr. Panayotis Verginis for giving me the opportunity to fulfill my Master Thesis in his lab and for his constant support. His mentorship and guidance were invaluable and crucial for the research project. In addition, I am grateful to Aikaterini Hatzioannou, Aggelos Banos and Themis Alissafi for their consultation and help in everything I needed. Also, I must thank Dr. Boumpas and Maria Grigoriou for the collaboration and feedback, during the year. Special thanks go to my fellow Master and labmates Lydia Kalafati and Marina Anastasiou for assisting me, advising me and making these years productive, stimulating and beautiful. Finally, I feel obligated to thank Dr. Bertias and Dr. Sidiropoulos for participating in the evaluation of this project.

References

1. Σκορίλας, Α., *Αρχές Κλινικής Χημείας και Μοριακής Δοαγνωστικής*, ed. Ε. Συμμετρία. 2009.
2. Hanahan, D. and R.A. Weinberg, *Hallmarks of cancer: the next generation*. Cell, 2011. **144**(5): p. 646-74.
3. Chen, D.S. and I. Mellman, *Oncology meets immunology: the cancer-immunity cycle*. Immunity, 2013. **39**(1): p. 1-10.
4. Gabrilovich, D.I. and S. Nagaraj, *Myeloid-derived suppressor cells as regulators of the immune system*. Nat Rev Immunol, 2009. **9**(3): p. 162-74.
5. Youn, J.I., et al., *Subsets of myeloid-derived suppressor cells in tumor-bearing mice*. J Immunol, 2008. **181**(8): p. 5791-802.
6. Hatzioannou, A., T. Alissafi, and P. Verginis, *Myeloid-derived suppressor cells and T regulatory cells in tumors: unraveling the dark side of the force*. J Leukoc Biol, 2017. **102**(2): p. 407-421.
7. Khaled, Y.S., B.J. Ammori, and E. Elkord, *Myeloid-derived suppressor cells in cancer: recent progress and prospects*. Immunol Cell Biol, 2013. **91**(8): p. 493-502.
8. Kumar, V., et al., *CD45 Phosphatase Inhibits STAT3 Transcription Factor Activity in Myeloid Cells and Promotes Tumor-Associated Macrophage Differentiation*. Immunity, 2016. **44**(2): p. 303-15.
9. Nagaraj, S., et al., *Antigen-specific CD4(+) T cells regulate function of myeloid-derived suppressor cells in cancer via retrograde MHC class II signaling*. Cancer Res, 2012. **72**(4): p. 928-38.
10. Osborne, T.J.K.R.A.G.B.A., *Kuby Immunology*, ed. W.H.F.a. Company. 2007.
11. Neefjes, J., et al., *Towards a systems understanding of MHC class I and MHC class II antigen presentation*. Nat Rev Immunol, 2011. **11**(12): p. 823-36.
12. Mizushima, N., *Autophagy: process and function*. Genes Dev, 2007. **21**(22): p. 2861-73.
13. Deretic, V., T. Saitoh, and S. Akira, *Autophagy in infection, inflammation and immunity*. Nat Rev Immunol, 2013. **13**(10): p. 722-37.
14. Crozter, V.L. and J.S. Blum, *Autophagy and adaptive immunity*. Immunology, 2010. **131**(1): p. 9-17.

15. Pouyssegur, J., F. Dayan, and N.M. Mazure, *Hypoxia signalling in cancer and approaches to enforce tumour regression*. Nature, 2006. **441**(7092): p. 437-43.
16. Azad, M.B., et al., *Hypoxia induces autophagic cell death in apoptosis-competent cells through a mechanism involving BNIP3*. Autophagy, 2008. **4**(2): p. 195-204.
17. Schaaf, M.B., et al., *The autophagy associated gene, ULK1, promotes tolerance to chronic and acute hypoxia*. Radiother Oncol, 2013. **108**(3): p. 529-34.
18. Mazure, N.M. and J. Pouyssegur, *Hypoxia-induced autophagy: cell death or cell survival?* Curr Opin Cell Biol, 2010. **22**(2): p. 177-80.
19. Corzo, C.A., et al., *HIF-1alpha regulates function and differentiation of myeloid-derived suppressor cells in the tumor microenvironment*. J Exp Med, 2010. **207**(11): p. 2439-53.
20. Liu, G., et al., *SIRT1 limits the function and fate of myeloid-derived suppressor cells in tumors by orchestrating HIF-1alpha-dependent glycolysis*. Cancer Res, 2014. **74**(3): p. 727-37.
21. Melero, I., et al., *T-cell and NK-cell infiltration into solid tumors: a key limiting factor for efficacious cancer immunotherapy*. Cancer Discov, 2014. **4**(5): p. 522-6.
22. Bos, R. and L.A. Sherman, *CD4+ T-cell help in the tumor milieu is required for recruitment and cytolytic function of CD8+ T lymphocytes*. Cancer Res, 2010. **70**(21): p. 8368-77.
23. Marzo, A.L., et al., *Tumor-specific CD4+ T cells have a major "post-licensing" role in CTL mediated anti-tumor immunity*. J Immunol, 2000. **165**(11): p. 6047-55.
24. Muranski, P., et al., *Tumor-specific Th17-polarized cells eradicate large established melanoma*. Blood, 2008. **112**(2): p. 362-73.
25. Martin-Orozco, N., et al., *T helper 17 cells promote cytotoxic T cell activation in tumor immunity*. Immunity, 2009. **31**(5): p. 787-98.
26. Poschke, I., et al., *Immature immunosuppressive CD14+HLA-DR-/low cells in melanoma patients are Stat3hi and overexpress CD80, CD83, and DC-sign*. Cancer Res, 2010. **70**(11): p. 4335-45.
27. Zea, A.H., et al., *Arginase-producing myeloid suppressor cells in renal cell carcinoma patients: a mechanism of tumor evasion*. Cancer Res, 2005. **65**(8): p. 3044-8.
28. Delamarre, L., et al., *Differential lysosomal proteolysis in antigen-presenting cells determines antigen fate*. Science, 2005. **307**(5715): p. 1630-4.

29. Kimmelman, A.C., *The dynamic nature of autophagy in cancer*. Genes Dev, 2011. **25**(19): p. 1999-2010.
30. White, E., *The role for autophagy in cancer*. J Clin Invest, 2015. **125**(1): p. 42-6.
31. Towers, C.G. and A. Thorburn, *Therapeutic Targeting of Autophagy*. EBioMedicine, 2016. **14**: p. 15-23.